bioRxiv preprint doi: https://doi.org/10.1101/481721; this version posted November 29, 2018. The copyright holder for this preprint (which was not certified by peer review) is the author/funder, who has granted bioRxiv a license to display the preprint in perpetuity. It is made available under aCC-BY-ND 4.0 International license.

1

2

3

4 The *Drosophila fussel* gene is required for bitter gustatory neuron differentiation

5 acting within an Rpd3 dependent chromatin modifying complex

6

7 Mathias Rass*, Svenja Oestreich, Severin Guetter, Susanne Fischer and Stephan

8 Schneuwly

9

10 Department of Developmental Biology, Institute of Zoology, University of

11 Regensburg, Regensburg, Bavaria, Germany

12

13 *Corresponding author

14 Email: mathias.rass@ur.de

15

16

17

18

19

20

bioRxiv preprint doi: https://doi.org/10.1101/481721; this version posted November 29, 2018. The copyright holder for this preprint (which was not certified by peer review) is the author/funder, who has granted bioRxiv a license to display the preprint in perpetuity. It is made available under aCC-BY-ND 4.0 International license.

21 **Abstract**

22 Members of the Ski/Sno protein family are classified as proto-oncogenes and act as
23 negative regulators of the TGF-ß/BMP-pathways in vertebrates and invertebrates. A
24 newly identified member of this protein family is *fussel* (*fuss*), the *Drosophila*
25 homologue of the human *functional Smad suppressing elements* (*fussel-15* and
26 *fussel-18*). We and others have shown that Fuss interacts with SMAD4 and that
27 overexpression leads to a strong inhibition of Dpp signaling. However, to be able to
28 characterize the endogenous Fuss function in *Drosophila melanogaster,* we have
29 generated a number of state of the art tools including anti-Fuss antibodies, specific
30 *fuss*-Gal4 lines and *fuss* mutant fly lines via the CRISPR/Cas9 system. Fuss is a
31 predominantly nuclear, postmitotic protein, mainly expressed in interneurons and *fuss*
32 mutants are fully viable without any obvious developmental phenotype. To identify
33 potential target genes or cells affected in *fuss* mutants, we conducted targeted
34 DamID experiments in adult flies, which revealed the function of *fuss* in bitter
35 gustatory neurons. We fully characterized *fuss* expression in the adult proboscis and
36 by using food choice assays we were able to show that *fuss* mutants display defects
37 in detecting bitter compounds. This correlated with a reduction of gustatory receptor
38 gene expression (Gr33a, Gr66a, Gr93a) providing a molecular link to the behavioral
39 phenotype. In addition, Fuss interacts with Rpd3, and downregulation of *rpd3* in
40 gustatory neurons phenocopies the loss of Fuss expression. Surprisingly, there is no
41 colocalization of Fuss with phosphorylated Mad in the larval central nervous system,
42 excluding a direct involvement of Fuss in Dpp/BMP signaling.

43 Here we provide a first and exciting link of Fuss function in gustatory bitter neurons.
44 Although gustatory receptors have been well characterized, little is known regarding
45 the differentiation and maturation of gustatory neurons. This work therefore reveals

bioRxiv preprint doi: https://doi.org/10.1101/481721; this version posted November 29, 2018. The copyright holder for this preprint (which was not certified by peer review) is the author/funder, who has granted bioRxiv a license to display the preprint in perpetuity. It is made available under aCC-BY-ND 4.0 International license.

46 Fuss as a pivotal element for the proper differentiation of bitter gustatory neurons
47 acting within a chromatin modifying complex.

48 Introduction

49 During development, the TGF-ß superfamily plays an important role in cell
50 proliferation, differentiation, apoptosis, cell adhesion, wound healing, bone
51 morphogenesis and cell motility [1]. Accordingly, there are multiple inhibitory factors
52 taking care of proper regulation of TGF-ß pathways. Besides inhibitory Smads and
53 Smurfs, which act by preventing the activation of TGF-ß receptors, another group of
54 negative regulators of the TGF-ß pathway exists: The Ski/Sno protein family [2–4].
55 Although Ski/Sno proteins are classified as proto-oncogenes, their exact role in
56 cancer progression is not fully understood. Various experimental approaches have
57 identified pro- and anti-oncogenic features, where the tumor promoting function of
58 Ski/Sno proteins seems to be mainly linked to their ability to counteract the anti-
59 proliferative effects of TGF-ß signaling [5,6]. Physiologically, Ski and Sno have both
60 been implicated in axonal morphogenesis, myogenesis and mammary gland
61 alveogenesis [7–9]. Proteins of the Ski/Sno family are characterized by a Ski/Sno
62 homology domain and a SMAD4 binding domain. These domains, although
63 resembling DNA binding domains, mediate protein-protein interactions enabling
64 binding of mSin3a, N-CoR, the histone deacetylase HDAC1, SMAD4 and different
65 regulatory SMADs, thus leading to the recruitment of a repressive transcription
66 complex, binding to target genes of the TGF-ß signaling pathway [10–12].

67 Whereas Ski and Sno are expressed mainly ubiquitously, two additional members of
68 the Ski/Sno protein family, the functional smad suppressing elements (Fussel) 15 and
69 18 (Skor1 and Skor2 in mouse, respectively), are highly restricted to postmitotic
70 neurons such as Purkinje cells [13–15]. Previous analysis showed that Skor1

bioRxiv preprint doi: https://doi.org/10.1101/481721; this version posted November 29, 2018. The copyright holder for this preprint (which was not certified by peer review) is the author/funder, who has granted bioRxiv a license to display the preprint in perpetuity. It is made available under aCC-BY-ND 4.0 International license.

71 interacts with Smad3 and acts as a transcriptional corepressor for LBX1, whereas
72 Skor2 inhibits BMP signaling in overexpression assays and is required for the
73 expression of Sonic Hedgehog in Purkinje cells. In addition, Skor2 is needed for
74 proper differentiation of Purkinje cells and knockout mice die prematurely within 24 h
75 after birth. However, there is no further insight into the functional mechanisms of
76 Skor1 in mice [15–17].

77 In contrast to vertebrates, *Drosophila melanogaster* has only two Ski/Sno proteins:
78 The Ski novel oncogene Snoo and the functional Smad suppressing element Fussel
79 (Fuss). Snoo is the homologue of Ski and Sno and Fuss the homologue of Skor1 and
80 Skor2. As in mice, Snoo is expressed broadly during development and adulthood,
81 whereas Fuss expression is limited to a subset of cells in the nervous system during
82 development [18]. Snoo has been found to be involved in eggshell patterning and in
83 wing and tracheal development in *Drosophila melanogaster* [19–21]. Recent findings
84 of Fuss function are highly controversial due to the lack of a reliable *Drosophila fussel*
85 mutation. Loss of function experiments with a chromosomal deletion suggested, that
86 Fuss acts as a cofactor for Smox signaling enabling ecdysone receptor (EcRB1)
87 expression in developing mushroom bodies in the brain. In addition, a severe
88 malformation of the adult mushroom bodies was detected [22]. Contrary to these
89 results, in overexpression assays Fuss leads to an inhibition of BMP signaling via its
90 interaction with Medea, the SMAD4 homologue in *Drosophila melanogaster* [18].

91 To clarify the molecular and physiological function of Fuss, we generated a complete
92 loss of function allele via CRISPR/Cas9 editing. Interestingly, *fuss* mutants are fully
93 viable, suggesting a modulatory function during development or/and adulthood,
94 rather than an essential role for cell survival. To be able to better analyze Fuss
95 expressing cells, we generated specific antibodies and reporter lines, which enabled

bioRxiv preprint doi: https://doi.org/10.1101/481721; this version posted November 29, 2018. The copyright holder for this preprint (which was not certified by peer review) is the author/funder, who has granted bioRxiv a license to display the preprint in perpetuity. It is made available under aCC-BY-ND 4.0 International license.

96 us to further clarify the expression pattern of Fuss. During development, Fuss is
97 expressed postmitotically in a highly restricted number of interneurons of the central
98 nervous system (CNS). In our *fuss* mutant, we could show that Fuss, in contrast to
99 previous studies, is neither acting as a negative regulator of BMP signaling
100 endogenously, nor involved in mushroom body development. A targeted DamID
101 (TaDa) experiment could not only confirm our findings molecularly, but also revealed,
102 that Fuss is expressed in bitter sensory neurons. In consequence, *fuss* mutant flies
103 lack the ability to sense bitter compounds and show reduced expression of bitter
104 gustatory receptors. Furthermore, interaction studies show that Fuss can form a
105 protein complex with Rpd3, a homologue of HDAC1, and indeed, downregulation of
106 *rpd3* in bitter gustatory neurons resembles loss of Fuss. Thus, we propose that the
107 Fuss/Rpd3 complex is required for proper cell fate determination in gustatory neurons
108 either by direct or indirect control of the expression of gustatory bitter sensing
109 receptors.

110 ## Results

111 ### Generation and analysis of *fuss* mutants

112 The *fuss* gene is localized on the fourth chromosome and therefore, due to the
113 limited genetic resources for this chromosome, *fuss* mutations have escaped
114 discovery in genetic screens for developmental mutations and previous research on
115 this gene focused either on overexpression studies or on a chromosomal deletion
116 covering multiple genes [18, 22]. However, it was shown recently that genes of the
117 fourth chromosome can be CRISPR/Cas9 edited via homology directed repair and
118 thus, we decided to generate a *fuss* null allele using this system [23]. A prerequisite
119 for proper mutant generation is a detailed analysis of the genomic organisation of the
120 gene. The *fuss* gene locus is fairly complex as it overlaps N-terminally with the RNA

bioRxiv preprint doi: https://doi.org/10.1101/481721; this version posted November 29, 2018. The copyright holder for this preprint (which was not certified by peer review) is the author/funder, who has granted bioRxiv a license to display the preprint in perpetuity. It is made available under aCC-BY-ND 4.0 International license.

121 gene *sphinx* and C-terminally with the RNA gene *CR44030*. In addition, the Pax6
122 homologue *twin of eyeless* (*toy*) lies downstream of *fuss* and is transcribed in the
123 opposite direction. Although the two genes are over 10 kb away from each other,
124 regulatory sites of *toy* are located in the vicinity of the transcription start site of *fuss*
125 [24].

126 Three different transcriptional start sites of *fuss* are annotated, which lead to three
127 transcripts *fussB*, *fussC* and *fussD*. *FussB* and *fussD* have an identical amino acid
128 sequence in contrast to the *fussC* transcript, which differs in 25 amino acids N-
129 terminally from *fussB* and *fussD*. *FussC* uses an artificial promoter sequence due to a
130 transposon insertion, leading to the assumption that this transcript is rather
131 insignificant as it is of very low abundance (see below). To reduce side effects by
132 deleting a silencer/enhancer structure of *sphinx* or *toy* and to maximise the effect on
133 *fuss,* we removed an 855bp fragment, which is shared by all three transcripts (Fig
134 1A). This fragment contains the conserved Ski/Sno/Dac homology and SMAD4
135 binding domains, which are important for protein interactions and function of the
136 Ski/Sno proteins [25,26]. Simultaneously, an attP site was introduced in the open
137 reading frame of all *fuss* transcripts, which additionally results in a premature stop
138 codon. Successful deletion of the two domains and the presence of the attP site was
139 confirmed by PCR and subsequent DNA sequencing (S1A Fig). We termed this
140 deletion *fuss*^{delDS} and it is a null allele. Due to the deletion and the premature stop
141 codon no functional proteins can be made, which could be shown by anti-Fuss
142 antibody stainings of heterozygous and homozygous *fuss*^{delDS} embryos (S1B Fig and
143 S1C Fig). As a second mutant allele, we used the MiMIC-line *fuss*^{Mi13731}, which is a
144 gene trap insertion leading to the expression of GFP under the *fussB* and *fussD*
145 promotor and a premature transcriptional stop of the *fussB* and *fussD* transcripts (Fig
146 1A). qPCR revealed that transcript levels of *fussB* and *fussD* in homozygous

bioRxiv preprint doi: https://doi.org/10.1101/481721; this version posted November 29, 2018. The copyright holder for this preprint (which was not certified by peer review) is the author/funder, who has granted bioRxiv a license to display the preprint in perpetuity. It is made available under aCC-BY-ND 4.0 International license.

147 *fuss*^{Mi13731} flies are reduced to ten percent in contrast to WTB flies (S1D Fig). With an
148 anti-GFP and anti-Fuss antibody staining, we could confirm that heterozygous
149 *fuss*^{Mi13731}/+ flies express GFP in the correct Fuss expression pattern, whereas Fuss
150 staining in homozygous *fuss*^{Mi13731} flies is reduced to background levels (S1E Fig and
151 S1F Fig). We conclude that *fuss*^{Mi13731} is at least a strong hypomorph for *fuss*, which
152 further suggests that *fussC* is not specifically expressed or only at very low levels. In
153 addition to *fuss*^{Mi13731}, which can be used as a GFP reporter line, we created a Gal4
154 line from *fuss*^{Mi13731} by recombination mediated cassette exchange [27]. This Gal4
155 line was named *fussBD*-Gal4 and it was edited with the CRISPR/Cas9 system
156 following the same strategy as for the *fuss*^{delDS} allele. This resulted in a line called
157 *fuss*^{delDS}-Gal4, which allows Gal4 expression in Fuss expressing cells in a mutant
158 background enabling us to analyze the presence and integrity of these cells. At last,
159 we generated a UAS-*t::gRNA-fuss*^{4x}, which allows cell specific gene disruption of
160 *fuss* via the UAS-Gal4 system [28]. The gRNAs target four CRISPR target sites
161 located in the DNA sequence of the Ski/Sno homology domain (S1G Fig). We could
162 detect a strong loss of GFP signal in adult brains of flies overexpressing GFP tagged
163 Fuss, Cas9 and *t::gRNA-fuss*^{4x} by *fussBD*-Gal4 compared to adult brains only
164 expressing GFP tagged Fuss and Cas9 by *fussBD*-Gal4 (S1H and S1I Fig).
165 In a previous study by Takaesu et al. [22], a 40 kb spanning genomic deletion
166 including the *fuss* gene (among several other genes) was used for functional studies
167 of the *fuss* gene. They observed a strongly reduced survivability during development
168 and a decreased lifespan, which was attributed to the loss of Fuss expression alone.
169 In contrast to their results, we did not observe a reduced survivability during larval or
170 pupal stages with our *fuss* mutant flies. Therefore, we conducted longevity
171 experiments. Neither homozygous *fuss*^{Mi13731} nor *fuss*^{delDS}–flies showed a significant
172 reduction in lifespan compared to their controls (Fig 1B and Fig 1C).

bioRxiv preprint doi: https://doi.org/10.1101/481721; this version posted November 29, 2018. The copyright holder for this preprint (which was not certified by peer review) is the author/funder, who has granted bioRxiv a license to display the preprint in perpetuity. It is made available under aCC-BY-ND 4.0 International license.

173 Next, we compared the CD8-GFP expression pattern of heterozygous *fuss*^{delDS}-
174 Gal4/+ and mutant *fuss*^{delDS}-Gal4/*fuss*^{delDS} flies. We did neither observe an evident
175 loss of GFP positive cells in the CNS of third instar larvae (Fig 1D and Fig 1E) nor in
176 three to five-day old adult flies (Fig 1F and Fig 1G). Therefore, loss of fuss does
177 neither lead to cell death, nor to a reduced survival during development or to a
178 shortened lifespan.

179 **Characterization of embryonic Fuss expressing cells reveals distinct neuronal**
180 **identities**

181 Due to the absence of any clear visible phenotype, we created specific polyclonal
182 antibodies against a 16 kDa nonconserved fragment localized at the C-terminus of
183 Fuss to characterize Fuss expressing cells and to draw conclusions about its function
184 (S2A Fig). These anti-Fuss antibodies clearly detect a Fuss-GFP fusion protein on
185 western blots and stainings mirror previously conducted RNA *in situ* hybridisations
186 (S2B Fig) [18, 22].

187 In a first overview of Fuss staining during embryonic development, Fuss expression
188 is mainly observed in the embryonic brain (Fig 2A, circles), the developing
189 stomatogastric nervous system (Fig 2A, arrowhead), single cells lying anterior to the
190 CNS (Fig 2A arrows), which will develop to inner gustatory neurons as shown later
191 and the ventral nerve cord (VNC, Fig 2B). As Fuss is characterized by its conserved
192 domains as a member of the Ski/Sno protein family, which are all considered to be
193 transcription regulators, we observe Fuss protein, as expected, exclusively localized
194 in the nucleus. During embryonic development, Fuss protein appears first at stage 13
195 and the number of Fuss positive cells increases continuously from early to late
196 embryonic stages as previously observed (S2C Fig [22]). At embryonic stage 16,
197 expression can be observed in two to five cells per hemineuromer with ascending
198 numbers from posterior to anterior (Fig 2B and S2C Fig).

bioRxiv preprint doi: https://doi.org/10.1101/481721; this version posted November 29, 2018. The copyright holder for this preprint (which was not certified by peer review) is the author/funder, who has granted bioRxiv a license to display the preprint in perpetuity. It is made available under aCC-BY-ND 4.0 International license.

199 The late appearance of the Fuss protein during development suggested, that Fuss
200 might be expressed only postmitotically. We confirmed this hypothesis by visualizing
201 ganglion mother cells in the embryo with anti-Prospero and Fuss cells with anti-Fuss
202 antibodies and no overlapping stainings were detected (Fig 2C). As shown by
203 colocalization studies with the glia marker Repo and the neuronal marker Elav, the
204 staining pattern is exclusively neuronal (Fig 2D). To further identify neuronal
205 subpopulations in hemineuromers of the VNC, prominent neuronal markers such as
206 Engrailed (En), Even skipped (Eve), Apterous (Ap), Hb9, Dachshund (Dac) and Twin
207 of eyeless (Toy) were utilised. No colocalization of Fuss with the interneuron marker
208 En or with the motoneuron markers Eve or Hb9 was observed (S2D Fig, S2E Fig and
209 S2F Fig). Because Eve and Hb9 label most of the embryonic motoneurons, Fuss is
210 unlikely to be expressed in motoneurons [29,30]. We were especially interested if
211 Dac and Fuss colocalize, because the interneuron marker Dac shares sequence
212 similarity with Ski and Sno and consequently is a related protein to Fuss [31,32].
213 Interestingly, Dac and Fuss are partially coexpressed, which emphasizes that at least
214 some Fuss neurons are interneurons (arrowhead, Fig 2E and Fig 2F). As the Toy
215 gene lies only 11 kb downstream of Fuss as it is transcribed in the opposite direction,
216 it is reasonable that they partially share enhancer/silencer regions. Remarkably, we
217 only found one Toy positive Fuss neuron per hemineuromer in the VNC (arrow, Fig
218 2E and Fig 2F) excluding extensive overlap of regulatory regions. Ap is expressed in
219 three cells per abdominal hemineuromer. These cells are subdivided into one dorsal
220 Ap and two ventral Ap interneurons [33]. Using the *ap*-tau-LacZ reporter, which only
221 labels one ventral Ap cell and the *ap*-Gal4 driver line we showed, that both ventral AP
222 interneurons are Fuss positive (Fig 2G and S2G Fig). Due to the location of the Toy
223 positive Fuss neuron, we assume that it is one of the ventral Ap cells and therefore
224 also an interneuron.

bioRxiv preprint doi: https://doi.org/10.1101/481721; this version posted November 29, 2018. The copyright holder for this preprint (which was not certified by peer review) is the author/funder, who has granted bioRxiv a license to display the preprint in perpetuity. It is made available under aCC-BY-ND 4.0 International license.

225 Taken together we could show that Fuss is expressed only postmitotically in
226 interneurons in the developing CNS, which will be further confirmed later.

227 **Transcriptional profiling of adult Fuss neurons in the head**

228 Fuss is expressed in heterogenic neuronal populations, which are represented by
229 differentially expressed markers and by their projection patterns. To develop new
230 approaches to identify and study viable phenotypes in *fuss* mutants, it was of upmost
231 importance to identify genes, which are regulated by Fuss. Therefore, we performed
232 a targeted DamID (TaDa) experiment by expressing a Dam-PolII fusion protein with
233 the *fuss*^{delDS}-Gal4 driver line. RpII215, the large subunit of the RNA Polymerase II, is
234 fused with the Dam methylase and thus this so called Dam-PolII fusion protein
235 enabled us to detect the binding sites of the RNA Polymerase II similar to an RNA
236 PolII ChIP and to detect transcribed genes in these neurons without cell sorting [34].
237 As a control, the unfused Dam protein was expressed with the *fuss*^{delDS}-Gal4 driver
238 line. Expression of UAS-*Dam* or UAS-*Dam-PolII* was inhibited by Gal80ts during
239 development and expression of this proteins was allowed for 24 h at 29 °C in one to
240 three-day old flies. Next generation sequencing libraries were generated from three
241 different biological replicates expressing Dam-PolII and from three replicates
242 expressing Dam alone. Each experiment was compared to each control leading to
243 nine individual datasets. Because the binding patterns of all nine files were highly
244 similar, individual datasets were averaged to reduce the amount of false positive hits
245 of expressed genes. Genes with a false discovery rate (FDR) lower than 0.01 were
246 accounted as expressed resulting in 2932 genes (S1 Appendix). The TaDa data is
247 represented as a log2 ratio of Dam-PolII/Dam. As expected, *fuss* was one of the
248 genes with the lowest FDR and highest PolII coverage (Fig 3A). This clearly indicates
249 that the approach was carried out successfully. Furthermore, genes already identified
250 by antibody stainings such as *elav*, *dac* or *toy*, were also detected by the TaDa

bioRxiv preprint doi: https://doi.org/10.1101/481721; this version posted November 29, 2018. The copyright holder for this preprint (which was not certified by peer review) is the author/funder, who has granted bioRxiv a license to display the preprint in perpetuity. It is made available under aCC-BY-ND 4.0 International license.

251 experiment. Toy was also expressed in some Fuss neurons in adult brains (Fig 3B).
252 This again underlines, like already observed during embryonic development, that *fuss*
253 and *toy* might share common silencer/enhancer elements with Fuss. To further verify
254 the TaDa data, colocalization experiments were conducted. Two cell fate markers
255 *atonal* (*ato*) and *acj6* were enriched in our dataset and we could also detect the
256 expression of these two proteins via immunofluorescense stainings in Fuss neurons
257 (Fig 3B). Furthermore, we analyzed *genes* which show no or low PolII coverage e.g.
258 *pale* (*ple*) and *Insulin-like peptide 2* (*Ilp2*) via immunofluorescence and could not
259 detect any staining in Fuss positive neurons (S3 Fig). In particular, the absence of
260 Fuss in insulin producing cells is in disagreement with recent published results using
261 enhancer/reporter constructs (S3B Fig, [35,36]). In summary, we can conclude, that
262 using this strategy, we have successfully generated an adult Fuss neuron specific
263 transcriptional profile.
264 In the next step, we wanted to search for potential target genes of Fuss using the
265 same strategy and conditions as above, but this time *fuss*^{delDS}-Gal4 was kept over the
266 *fuss*^{delDS} allele to profile transcription of *fuss* mutant neurons. Again, individual
267 datasets were averaged and genes with an FDR lower than 0.01 were accounted as
268 expressed resulting in 3150 genes (S2 Appendix). The comparison of the
269 log_2(DamPolII/Dam) data of heterozygous *fuss*^{delDS}/+ and homozygous *fuss*^{delDS} flies
270 showed, that there is not a strong deviation (coefficient of deviation $R^2 = 0.889$) of the
271 mutant transcriptional profile from the control (Fig 3C). Because Fuss is only
272 expressed in a small number of CNS neurons, the acquired data can only be
273 confirmed by antibody staining and not by semiquantitive qPCR or western blots from
274 whole heads. There were three genes which attracted our attention: *Eaat2*, *Ir76b* and
275 especially *Gr66a* as they provided a possible link to Fuss expression in gustatory
276 sense neurons (Fig 3D). These genes could be found in both datasets, although only

bioRxiv preprint doi: https://doi.org/10.1101/481721; this version posted November 29, 2018. The copyright holder for this preprint (which was not certified by peer review) is the author/funder, who has granted bioRxiv a license to display the preprint in perpetuity. It is made available under aCC-BY-ND 4.0 International license.

277 *Eaat2* had an FDR lower than 0.01 in both datasets. The PolII coverage of *Eaat2* and
278 *Ir76b* was only slightly different between homozygous and heterozygous flies,
279 whereas *Gr66a*, which is exclusively expressed in bitter gustatory sense neurons
280 (GRNs), showed a significant reduction in mutant flies (S1 Appendix and S2
281 Appendix).

282 **Fuss is expressed in a subset of gustatory neurons**

283 It has been shown that the glutamate aspartate transporter Eaat2 is expressed in
284 sensory neurons [37]. The ionotropic receptor Ir76b is expressed in gustatory
285 neurons and the gustatory receptor Gr66a is specifically expressed in bitter GRNs,
286 where Gr66a is a very important component for bitter taste sensation [38,39]. We
287 already observed Fuss expression in cells outside of the larval CNS, therefore, to
288 confirm the TaDa datasets, we analyzed gustatory neurons in larval and adult stages.
289 In larvae, Fuss expression cannot be observed in the terminal or dorsal organ, but it
290 can be found in the inner gustatory sense organs. We found Fuss expression in two
291 pairs of neurons in the dorsal pharyngeal sensilia (DPS, Fig 4A) one neuron pair in
292 the dorsal pharyngeal organ (DPO, Fig 4A) and two neuron pairs in the posterior
293 pharyngeal sensilia (PPS, Fig 4A). None of the GRNs in the ventral pharyngeal
294 sense organ (VPS) express Fuss. These cells have been already characterized by
295 expression of different gustatory receptors and we found that larval Fuss expressing
296 GRNs show a colocalization with a marker for bitter sensing neurons Gr33a [40]. In
297 addition, one neuron pair in the DPS also shows an overlap with Gr93a which has
298 been shown to be important for caffeine response in larvae (Fig 4B, [41,42]).

299 Later, in adulthood, Fuss expression continues in GRNs of the proboscis. In the adult
300 labellum three different types of sensilla can be found divided into short (S-type),
301 intermediate (I-type) and long sensilla (L-type). Intermediate sensilla are innervated
302 by two GRNs and short and long sensilla by four GRNs [43]. Interestingly Fuss

bioRxiv preprint doi: https://doi.org/10.1101/481721; this version posted November 29, 2018. The copyright holder for this preprint (which was not certified by peer review) is the author/funder, who has granted bioRxiv a license to display the preprint in perpetuity. It is made available under aCC-BY-ND 4.0 International license.

303 expression is observed in one GRN per gustatory sensilla and is consistently
304 colocalized with the bitter GRN marker Gr66a in neurons innervating short and
305 intermediate sensilia (Fig 4C [38]). Long sensilla do not contain a Gr66a positive
306 GRN, therefore, all Gr66a neurons in the labellum are Fuss positive, but not vice
307 versa. Another gustatory receptor which is broadly expressed and labels sweet
308 GRNs is Gr5a, but no overlap with Fuss positive neurons was observed (Fig 4D).
309 Besides Gr66a our TaDa dataset revealed that the ionotropic receptor Ir76b is
310 expressed in Fuss neurons. Ir76b has been shown to be expressed by one GRN per
311 L-type sensillum, which plays a role in attractive salt tasting [44]. We found that in L-
312 type sensilla Fuss is coexpressed with Ir76b (Fig 4E-G). Besides the expression in
313 GRNs of the proboscis we found Fuss being expressed in two GRNS each in the last
314 two tarsal segments in every leg (S4A Fig). In conclusion, we integrated Fuss
315 expression into the GRN model from Freeman and Dahanukar (Fig 4H, [45]) and
316 demonstrate that Fuss is expressed in bitter neurons in S- and I-type sensilla and in
317 salt attracting neurons in L-type sensilla.

318 **Loss of Fuss impairs bitter taste sensation**

319 By its gustatory system *Drosophila melanogaster* can discriminate between valuable
320 food sources for foraging or egg laying and toxic compounds which could harm the fly
321 or its offspring [46]. To address if Fuss is required for the proper development of
322 GRNs, we focused on the impact of Fuss mutation on differentiation of bitter GRNs,
323 because Fuss is expressed in all bitter GRNs of the proboscis. To detect if *fuss*
324 mutant flies display an impaired bitter taste sensation, we tested one to three-day old
325 flies in a two-choice feeding assay. In our standard test, flies had to choose between
326 1mM sucrose or 5mM sucrose plus 10mM caffeine. We calculated a preference index
327 ranging from zero to one, where zero indicates complete avoidance of the bitter
328 compound and one a complete preference for it, due to the higher sugar

bioRxiv preprint doi: https://doi.org/10.1101/481721; this version posted November 29, 2018. The copyright holder for this preprint (which was not certified by peer review) is the author/funder, who has granted bioRxiv a license to display the preprint in perpetuity. It is made available under aCC-BY-ND 4.0 International license.

329 concentration. First, Fuss expressing neurons were ablated by UAS-*rpr* expression
330 with *fussBD*-Gal4 to show their importance in bitter sensing and indeed, these flies
331 showed a strong impairment of bitter discrimination (Fig 5A). Furthermore,
332 homozygous *fuss*^{Mi13731}, *fuss*^{delDS} and transheterozygous mutants
333 (*fuss*^{Mi13731}/*fuss*^{delDS}) as well as their appropriate controls were tested. All mutant
334 genotypes showed an increased preference for 5mM sucrose mixed with caffeine
335 and by overexpression of Fuss in *fuss* mutant neurons we could revert preference to
336 wildtype levels (Fig 5A). To show that the behavioural phenotype of *fuss* mutants is
337 due to defects in GRNs and not derived from other higher order Fuss neurons in the
338 CNS we specifically disrupted *fuss* in all GRNs with the *Poxn*-Gal4-13-1 driverline
339 and our UAS-*cas9*; UAS-*t::gRNA-fuss*^{4x} flies. *Poxn*-Gal4-13-1 expresses Gal4 early
340 in development in all GRNs and in ellipsoid body neurons as well as interneurons of
341 the antennal lobe of the brain (Fig S4B, [47]), therefore the only common neuronal
342 populations between Fuss and *Poxn*-Gal4-13-1 are the GRNs and indeed, as shown
343 in Fig 5A, these flies show the same bitter sensing deficits. We also tested different
344 concentrations of caffeine as well as another bitter compound (denatonium benzoate)
345 and *fuss*^{Mi13731} flies always displayed a higher preference towards the 5mM sucrose
346 mixed with the bitter compound than controls except when concentration of the bitter
347 compound was too high (S4C and S4D Fig). Thus, not only detection of caffeine but
348 more general bitter sensation is disturbed, because different GR multimers are
349 needed for the detection of different aversive compounds, e.g. Gr93a which is
350 expressed in a subset of S-type sensilla is needed for caffeine but not for denatonium
351 benzoate sensation [48]. The gustatory receptor *Gr66a* showed a strong reduction in
352 PolII coverage in mutant flies in contrast to control flies and is only expressed in a
353 proportion of Fuss positive GRNs. The gustatory receptor GR33a has been found to
354 be coexpressed with Gr66a in bitter GRNs and both are involved in bitter sensation,

bioRxiv preprint doi: https://doi.org/10.1101/481721; this version posted November 29, 2018. The copyright holder for this preprint (which was not certified by peer review) is the author/funder, who has granted bioRxiv a license to display the preprint in perpetuity. It is made available under aCC-BY-ND 4.0 International license.

355 particularly together with Gr93a in caffeine sensation [40,48]. To validate GRN results
356 from the TaDa experiment, we extracted RNA from adult proboscis and analysed the
357 expression levels of those GRs via semiquantitative RT-PCR. In homozygous
358 *fuss*^{Mi13731}-flies Gr33a and Gr66a expression were strongly reduced as compared to
359 WTB and heterozygous *fuss*^{Mi13731}-flies. Gr93a expression levels of homozygous
360 *fuss*^{Mi13731}-flies were similar to WTB levels but reduced when compared to
361 heterozygous *fuss*^{Mi13731}-flies (Fig. 5B). The observed effects were enhanced in
362 *fuss*^{delDS}-flies. Gr33a, Gr66a and Gr93a expression levels were all reduced in
363 *fuss*^{delDS}-flies in contrast to both controls (Fig. 5C). A similar downregulation of
364 Gr33a, Gr66a and Gr93a expression levels was observed in transheterozygous
365 *fuss*^{Mi13731}/*fuss*^{delDS} flies in contrast to WTB flies (S4E Fig). Next, we tested if the
366 number of Gr33a and Gr66a positive GRNs is reduced in *fuss* mutant flies. We
367 counted Fuss positive and Gr33a positive neurons in flies of the genotypes *Gr33a*-
368 Gal4/UAS-*LacZ*; *fuss*^{Mi13731}/+ and *Gr33a*-Gal4/UAS-*LacZ*; *fuss*^{Mi13731}/*fuss*^{delDS}. In this
369 genetic combination we counted 2.5 less Fuss positive cells and surprisingly 7.2 less
370 Gr33a positive cells in controls than in transheterozygous mutants (Fig 5D).
371 Furthermore, we analysed number of Fuss positive and Gr66a positive neurons in
372 flies of the genotypes UAS-*LacZ*/+; *Gr66a*-Gal4/+; *fuss*^{Mi13731}/+ and UAS-*LacZ*/+;
373 *Gr66a*-Gal4/+; *fuss*^{Mi13731}/*fuss*^{delDS}. We found the same reduction in overall number of
374 Fuss positive GRNs. But the number of Gr66a positive GRNs is decreased at the
375 same level as the number of overall Fuss positive GRNs (Fig 5E). Thus, the overall
376 number of bitter GRNs is slighty reduced in *fuss* mutant flies, but interestingly Gr33a
377 expression is completely abolished in some bitter GRNs, whereas the reduction of
378 Gr66a expression found in qPCR experiments does not result in a reduced number of
379 Gr66a positive GRNs. So, upon the loss of Fuss expression, bitter GRN

bioRxiv preprint doi: https://doi.org/10.1101/481721; this version posted November 29, 2018. The copyright holder for this preprint (which was not certified by peer review) is the author/funder, who has granted bioRxiv a license to display the preprint in perpetuity. It is made available under aCC-BY-ND 4.0 International license.

380 differentiation is highly disturbed, which renders these flies inable to detect bitter
381 compounds.

382 **Fuss interacts with the histone deacetylase Rpd3 to affect cell fate**
383 **determination**

384 In mammals there are two homologues of Fuss, Skor1 and Skor2, which display a
385 high sequence conservation within the Ski/Sno/Dac homology domain and the
386 SMAD4 binding domain. In contrast, the conservation in the C-terminal region is very
387 low, which shows a high degree of evolutionary divergence (S4F Fig). Although the I-
388 loop of the SMAD4 binding domain, which has been implicated as an important
389 structure for SMAD4 binding, is not very well conserved in Fuss and its homologues,
390 we and others have detected an interaction between SMAD4 with Fuss and Skor2,
391 respectively [11,14,18]. The repressive action of Ski/Sno proteins is generally exerted
392 by the recruitment of a protein complex containing HDAC1 [10]. Skor1 and Skor2
393 also interact with HDAC1 and interestingly, it has been shown that the residues
394 important for this interaction are localized in a segment reaching from amino acid
395 385-592 in mouse Skor2 [16,17]. Similar to the lack of the I-loop sequence, this
396 segment is highly diverse between Fuss and Skor2 challenging if Fuss nevertheless
397 is able to interact with Rpd3, the HDAC1 homologue in *Drosophila melanogaster*
398 (S4F Fig). Therefore, we performed Co-Immunoprecipitations (CoIP) and transfected
399 S2R+ cells with Fuss and Rpd3 tagged with FLAG or HA. Interaction between Fuss
400 and Rpd3 could be shown independent of the type of the tags (Fig 6A). Skor1 and
401 Skor2 have also been described to interact with Smad2 and Smad3, homologues of
402 the *Drosophila* Smox, which executes the same function as Mad, but in the TGF-ß
403 like signaling pathway [13,14,22]. Using the same methological approach as for the
404 Fuss and Rpd3 interaction, we could not detect any interaction between Fuss and
405 Smox, independent of the tags used (Fig 6A). Interestingly Smox is one of the genes

bioRxiv preprint doi: https://doi.org/10.1101/481721; this version posted November 29, 2018. The copyright holder for this preprint (which was not certified by peer review) is the author/funder, who has granted bioRxiv a license to display the preprint in perpetuity. It is made available under aCC-BY-ND 4.0 International license.

406 specifically enriched in our TaDa datasets for Fuss neurons, so there would be a
407 possibility for interaction in these cells.
408 If Fuss is acting within a protein complex in concert with Rpd3, we should be able to
409 mimic *fuss* mutant phenotypes with *rpd3* depletion. Therefore, a UAS-*rpd3*-IR
410 knockdown line was specifically expressed in Fuss neurons using the *fussBD*-Gal4
411 driver to reduce *rpd3* expression throughout development. Adult flies were then
412 tested again in a two-choice feeding assay for bitter sensing. *Rpd3* knockdown flies
413 showed a significant higher preference towards caffeine than control flies (*fussBD*-
414 Gal4 x UAS-*cherry*-IR; Fig 6B). Because Rpd3 is involved in many different
415 chromatin complexes, we analyzed again the expression levels of bitter gustatory
416 receptors. Expression of all three tested GRs Gr33a, Gr66a and Gr93a was again
417 diminished (Fig 6C) and therefore we conclude, that the Fuss/Rpd3 complex plays a
418 key role in the final cell fate determination of gustatory neurons.

419 **Fuss function in CNS neurons – a contentious issue**

420 In overexpression experiments, Ski/Sno proteins have often been identified as
421 negative regulators of TGF-ß or BMP-signaling [14,17]. In *Drosophila*, Dpp is the
422 main homologue to vertebrate BMPs and it is involved in multiple developmental
423 signaling events, in particular in the *Drosophila* wing [49]. We have previously shown,
424 that an overexpression of Fuss during wing development indeed results in diminished
425 expression of Dpp target genes and, concomitantly, induces a phenotype, which
426 resembles loss of Dpp signaling, despite the fact, that we could only detect a physical
427 interaction with the Co-Smad Medea but not with the R-Smad Mad [18]. In Dpp
428 signaling, Mad gets phosphorylated by the type I receptors Saxophon and/or Thick
429 veins and, thus phosphorylated Mad is an excellent marker for active Dpp signaling
430 and also for motoneurons or Tv neurons [50,51]. To analyse a possible role of Fuss
431 in Dpp signaling, we used *fuss*^{Mi13731}-flies, in which GFP is expressed under the *fuss*

bioRxiv preprint doi: https://doi.org/10.1101/481721; this version posted November 29, 2018. The copyright holder for this preprint (which was not certified by peer review) is the author/funder, who has granted bioRxiv a license to display the preprint in perpetuity. It is made available under aCC-BY-ND 4.0 International license.

432 promotor to label Fuss expressing cells and we counterstained 3rd instar larval brains
433 with an antibody against phosphorylated Mad (pMad) (Fig 7A and Fig 7B). These
434 results clearly showed that Fuss expression is not overlapping with pMad in
435 heterozygous *fuss*^{Mi1373}/+ conditions. As there is a possibility that Fuss is acting
436 upstream of Mad phosphorylation, we compared pMAD staining of heterozygous (Fig
437 7C) with homozygous *fuss*$^{Mi13731-}$flies (Fig 7D). Again, there is no overlap of pMAD
438 and GFP stainings in both genotypes, indicating that there is no increase of pMAD in
439 *fuss* mutant neurons in the absence of Fuss. Importantly, this is in agreement with
440 our overexpression studies, where Fuss had no influence on Mad phosphorylation
441 [18]. Therefore, we conclude, that endogenously Fuss is not involved in Dpp
442 signaling inhibition and it also emphasizes previous results, that Fuss is expressed in
443 interneurons and not in motoneurons, which require pMad activity [51].
444 Previously, the only loss of function data of *fuss* was generated using a genomic
445 deletion of 40 kb including the *fuss* locus and additional genes [22]. This deletion
446 lead to a reduced survivability during development, a shortened lifespan of the
447 escapers and an impaired mushroom body development. All these phenotypes were
448 attributed to the loss of Fuss expression. As we did not observe an impact on
449 survivability or lifespan upon the loss of Fuss (see above), we wondered if Fuss is
450 indeed involved in mushroom body development. Based on RNA *in situ*
451 hybridisations Takaesu et al. assumed that Fuss is expressed in Kenyon cells during
452 development and is required for the proper formation of the mushroom body [22].
453 Having now specific antibodies, gene trap constructs and *fuss* mutations in hand, we
454 decided to carefully reevaluate this data on mushroom body expression and function
455 during development. In a first step, we used *OK107*-Gal4 driven nuclear GFP as a
456 marker for developing Kenyon cells and colabeled larval brains with EcRB1 and
457 Fuss. We found that Fuss is not expressed in the developing mushroom body

bioRxiv preprint doi: https://doi.org/10.1101/481721; this version posted November 29, 2018. The copyright holder for this preprint (which was not certified by peer review) is the author/funder, who has granted bioRxiv a license to display the preprint in perpetuity. It is made available under aCC-BY-ND 4.0 International license.

458 Kenyon cells, but it shows a partial overlap with EcRB1 expression outside of the
459 Kenyon cell domain (Fig 7E-E´´´). Next, we analysed adult mushroom body
460 structures of *fuss* mutant flies using a FasII-antibody. As expected, due to the lack of
461 Fuss expression in Kenyon cells, no deformation or loss of any of the lobes of the
462 mushroom body was observed in homozygous $fuss^{Mi13731}$ or $fuss^{delDS}$-flies (Fig 7F-Fig
463 7I). In addition, the expression of *rpr* with the $fuss^{delDS}$-Gal4 line lead to a complete
464 ablation of Fuss neurons, but did not result in a malformation of adult mushroom
465 bodies (Fig 7J). Furthermore, expression of CD8-GFP with *fussBD*-Gal4 in adult
466 brains shows that Fuss neuron clusters are also localized distal to the mushroom
467 body (Fig 7K). In fact, Fuss neuronal projections are localized outside of the
468 mushroom body lobes in the adult brain and some Fuss neurons are targeting the
469 optic lobe including different layers of the medulla, lobula and lobula plate but not the
470 lamina (Fig 7L). From these results, we conclude that *fuss* has no impact on
471 mushroom body development and that most of these neuronal populations such as
472 the Fuss/Atonal positive neurons are higher order neurons of the visual system.

473 Discussion

474 The molecular and cellular functions of the *fuss* genes, which are members of the
475 Ski/Sno protein family, are still poorly understood. The fact that *Drosophila* contains
476 only one single *fuss* gene offers a great opportunity for a thorough analysis.
477 However, this has been restrained due to its location on the 4th chromosome, where
478 only limited genetic tools were available. As a consequence, previous reports have
479 been focusing on the analysis of either overexpression studies or by using a multi-
480 gene deficiency with contradictory results [18,22]. In the meantime, more recent
481 methodological advances like the CRISPR/Cas9 genome editing [52] and the MiMIC
482 gene trap technique [27] have expanded the *Drosophila* genetic toolbox and provided

bioRxiv preprint doi: https://doi.org/10.1101/481721; this version posted November 29, 2018. The copyright holder for this preprint (which was not certified by peer review) is the author/funder, who has granted bioRxiv a license to display the preprint in perpetuity. It is made available under aCC-BY-ND 4.0 International license.

483 an appropriate genetic environment allowing a thorough and in-depth study of such
484 genes. The availability of the *fuss*^{Mi13731} fly line, which is a gene trap of *fuss*, allowed
485 us to study the expression pattern of Fuss. This line perfectly matches our Fuss-
486 antibody stainings and was used to create a Gal4 line via RMCE as previously
487 described [27]. A second independent mutant *fuss* allele, *fuss*^{delDS} was created by
488 CRISPR/Cas9 editing by deletion of the main functional protein domains. Although
489 *fuss*^{Mi13731} and *fuss*^{delDS} alleles are generated by different genetic approaches they
490 share the same phenotypes, underlining that despite the complex genomic
491 organization of *fuss* the observed phenotypes are due to the loss of *fuss*.
492 Surprisingly, *fuss* mutant flies are fully viable and do neither show developmental
493 lethality or reduced lifespans nor any other apparent phenotypes.

494 By means of our new tools, we could show that Fuss is expressed postmitotically in a
495 small subset of neurons. All Fuss neurons in the CNS are interneurons, but they
496 express different cell fate markers, suggesting that they represent a rather diverse
497 group of neurons. These results were confirmed molecularly by a targeted DamID
498 experiment, which, in addition, indicated a highly specific expression of gustatory
499 receptor genes and indeed, Fuss is expressed in one GRN per sensillum. In S and I-
500 type sensilla it is expressed in bitter GRNs and in L-type sensilla, which lack bitter
501 GRNs, it is expressed in salt attracting GRNs. We investigated how the bitter GRNs
502 react to the loss of Fuss and interestingly, this leads to an impairment of bitter
503 sensation. Remarkably, this phenotype is correlated with a downregulation of bitter
504 gustatory receptors Gr33a, Gr66a and Gr93a and in some bitter GRNs of *fuss* mutant
505 flies no Gr33a expression can be observed anymore. The expression of Fuss in
506 sensory neurons during development, and the adult phenotype, suggest that Fuss is
507 needed for the proper maturation of these neurons and therefore is essential for bitter

bioRxiv preprint doi: https://doi.org/10.1101/481721; this version posted November 29, 2018. The copyright holder for this preprint (which was not certified by peer review) is the author/funder, who has granted bioRxiv a license to display the preprint in perpetuity. It is made available under aCC-BY-ND 4.0 International license.

508 GRN differentiation. As there is a possibility, that the bitter sensation phenotype
509 might be due to some higher order interneurons within the CNS, we generated a
510 specific UAS-*t::gRNA-fuss*^{4x} line to be able to perform cell type specific gene
511 knockouts. Indeed, using an independent driver line (*Poxn*-Gal4-13-1) expressed in
512 all GRNs, faithfully reproduced this phenotype indicating a direct association of bitter
513 sensation and GRN defects. In *fuss* mutant flies morphology of bitter GRNs was not
514 altered and cell number was just slightly changed compared to controls, while Gr33a
515 expression was completely lost in 40% of all bitter GRNs and Gr66a expression was
516 reduced in all GRNs, but was never completely absent from a bitter GRN. Therefore,
517 in *fuss* mutant flies bitter GRNs are correctly specified but the terminal differentiation
518 of this neurons is disturbed, which ultimately results in impaired bitter taste sensation.
519 This is comparable to Fuss neurons in the larval and adult CNS, where loss of Fuss
520 expression also did not have an impact on axonal projections or cell numbers and
521 thus not on initial specification of these neurons. This supports the idea, that Fuss is
522 required for fine tuning individual subgroups of neurons during development, a
523 phenotype, which resembles loss of Skor2 in mice, where it is dispensable for initial
524 Purkinje cell fate specification but is required for proper differentiation and maturation
525 of Purkinje cells [15]. It is very likely that other genes will also be affected by the loss
526 of Fuss, and the reduction of these gustatory receptors could lead to a cumulative
527 effect, as it has been shown that they act in heteromultimers where a multimeric
528 receptor consists of at least Gr66a, Gr33a and Gr93a, which are all required for
529 caffeine sensation [53,54]. Whereas over the years many studies have dissected the
530 function of single gustatory receptors, the complexes they establish, and genes which
531 are involved in more common topics like sensory neuron formation, less is known
532 about the differentiation and specification of subsets of GRNs [55–57]. To find further
533 genes involved in differentiation of bitter GRNs and to clarify the molecular

bioRxiv preprint doi: https://doi.org/10.1101/481721; this version posted November 29, 2018. The copyright holder for this preprint (which was not certified by peer review) is the author/funder, who has granted bioRxiv a license to display the preprint in perpetuity. It is made available under aCC-BY-ND 4.0 International license.

534 consequences of the *fuss* mutation in bitter GRNs we will conduct transcriptional
535 profiling experiments specifically in Fuss positive GRNs.

536 Using the TaDa method, we were curious to see if this method is sensitive enough to
537 pick up significant differences between *fuss* mutant and wildtype flies. This was
538 indeed the case for *GR66a*. However, in general, the performed TaDa experiments
539 showed only slight differences between mutant and control flies. This could be a
540 consequence of Fuss being expressed in heterogenic neuronal clusters. We showed,
541 that Fuss interacts with Rpd3, a histone deacetylase, and therefore, a chromatin
542 modifier, which is preferentially associated with inhibitory gene regulating complexes
543 [58]. This could be a common mechanism for Fuss in all Fuss expressing neurons.
544 However, different neuronal populations have different open and closed chromatin
545 and probably the Fuss/Rpd3 complex regulates different genes in different neuronal
546 populations, which could lead to the masking of differential gene expression by
547 individual neuronal cell groups. Additionally, although the TaDa technique functions
548 very well to generate transcriptional profiles without cell isolation, data is
549 nondirectional and at GATC fragment resolution, which decreases overall resolution.
550 To overcome these limitations experiments are on the way to unravel the function of
551 specific neuronal clusters as well as the function of *fuss* in these neuronal clusters,
552 and to specifically profile transcription of these clusters and changes upon loss of
553 *fuss*.
554

555 A careful analysis with our newly generated antibodies shows, that there is no
556 expression of Fuss in larval or adult Kenyon cells as has been postulated recently
557 [22]. To unequivocally show, that there is no requirement for Fuss in mushroom body
558 development, neither autonomously nor non-autonomously, Fuss expressing neurons

bioRxiv preprint doi: https://doi.org/10.1101/481721; this version posted November 29, 2018. The copyright holder for this preprint (which was not certified by peer review) is the author/funder, who has granted bioRxiv a license to display the preprint in perpetuity. It is made available under aCC-BY-ND 4.0 International license.

559 were ablated using a *fuss*-GAL4 line driving Reaper. Again, these flies, even without
560 any *fuss* expressing cells, are fully viable and do not show mushroom body defects.
561 Lastly, we also did not find any evidence of Fuss being expressed in insulin
562 producing neurons by our antibody staining or DamID experiments as shown recently
563 [36]. These discrepancies are most likely explained by the use of the specific
564 knockout line $fuss^{delDS}$, and the gene trap line $fuss^{Mi13731}$ in our case, whereas a 40 kb
565 genomic deletion *Df(4)dCORL* was used in Takaesu et al. [22] and Tran et al. [36].
566 This deletion covered the *fuss* locus as well as two more protein coding genes, *4E-T*
567 and *mGluR*, and three noncoding RNA genes, *CR45201*, *CR44030* and *sphinx*. Any
568 of these, or a combination of them, could be responsible for premature lethality or
569 mushroom body defects. One additional possible explanation for their mushroom
570 body defects in the deletion is an inappropriate fusion of a new transcriptional start
571 site or enhancer region from the *mGluR* upstream to the *toy* gene creating a weak
572 overexpression phenotype of toy in mushroom bodies, a phenotype, which has been
573 described already [59]. Indeed, very recently Tran et al. [35] described a slight
574 overexpression of Toy in their deficiency allele *Df(4)dCORL*.

575 We and others have shown that Ski/Sno protooncogenes have an inhibitory effect on
576 TGF-ß or BMP signaling in overexpression assays [18,60]. This is often associated
577 with the ability of Ski/Sno proteins to inhibit the antiproliferative effects of TGF-ß
578 signaling in cancer and to promote their progression [61]. However, in an
579 endogenous situation, Fuss is not expressed in cells, where the BMP/Dpp signaling
580 pathway is active. This is displayed by the absence of the motoneuron marker pMad
581 in Fuss neurons. Later in adulthood, Mad itself is also not specifically enriched in
582 Fuss expressing neurons according to the TaDa dataset, clearly pointing against a
583 function in BMP signalling. We also tested if Fuss is involved in the Activin signaling

bioRxiv preprint doi: https://doi.org/10.1101/481721; this version posted November 29, 2018. The copyright holder for this preprint (which was not certified by peer review) is the author/funder, who has granted bioRxiv a license to display the preprint in perpetuity. It is made available under aCC-BY-ND 4.0 International license.

584 cascade, but we could not detect an interaction between Fuss and Smox in CoIP
585 assays. However, we cannot rule out the possibility that the phosphorylated form of
586 Smox is interacting with Fuss or the Fuss/Med complex. But since both,
587 phosphorylated Smox and Fuss interact with Medea, we would potentially also get an
588 artificial interaction [18,62]. At least according to the TaDa dataset, Smox is
589 expressed in Fuss neurons. Unfortunately, there is currently no good marker
590 available to test for an activated TGF-ß signaling pathway in *Drosophila* cells, like an
591 antibody against phosphorylated Smox. What might be the main molecular
592 mechanism for Fuss? Although the Ski/Sno/Dac homology domain and the SMAD4
593 binding domain in Ski have DNA binding character, they mainly have been shown to
594 be involved in protein-protein interactions [11,63]. Furthermore, Ski/Sno proteins do
595 not possess an intrinsic catalytic activity, they rather act as recruiting proteins [2]. In
596 agreement, we could show that this is also the case for Fuss. Not only that Fuss
597 binds to Medea, which is a DNA binding protein and therefore mediates the DNA
598 binding, Fuss also interacts with Rpd3, a histone deacetylase. Thus, the
599 Med/Fuss/Rpd3 complex is involved in chromatin silencing and plays a key role in
600 terminal differentiation. Interestingly, the loss of bitter sensation and downregulation
601 of bitter GRs could also be phenocopied by a knockdown of *rpd3* in Fuss expressing
602 gustatory neurons. One current hypothesis of Fuss/Rpd3 function in GRNs, which we
603 propose, is, that this protein complex is inhibiting a repressor of GR genes and in the
604 absence of either *fuss* or *rpd3*, the complex is inactivated, this repressor will inhibit
605 bitter GR genes.

606 For Ski and Sno, the transcriptional repressor complexes have been reasonably well
607 characterized [10,64], but for the Fuss-type proteins, very little is known about their
608 complexes. It would be highly interesting if Fuss proteins act through repressor

bioRxiv preprint doi: https://doi.org/10.1101/481721; this version posted November 29, 2018. The copyright holder for this preprint (which was not certified by peer review) is the author/funder, who has granted bioRxiv a license to display the preprint in perpetuity. It is made available under aCC-BY-ND 4.0 International license.

609 complexes identical to the complexes of Ski or Sno or a rather unique one. The most
610 exciting question to solve regarding protein interaction will be, if the Fuss/Rpd3
611 complex plays a role in TGF-ß signalling, or if in contrast to its mammalian
612 homologues, it is not only acting BMP independent, but also independent from the
613 TGF-ß signalling cascade. Besides identifying further protein-protein interactions and
614 investigating DNA-protein interactions more precisely, it will be very important to
615 describe the exact function of the Fuss/Rpd3 complex. In mammals, Skor2 is thought
616 to activate Sonic Hedgehog expression in Purkinje cells from direct binding to the
617 Sonic Hedgehog promotor and this might be achieved by inhibition of the BMP
618 pathway or by cooperation with the RORalpha pathway, a nuclear orphan receptor
619 [15,17]. In contrast to that, Skor1 interacts with Lbx1, a homologue of the ladybird
620 early or ladybird late in *Drosophila*, and acts as a transcriptional corepressor of Lbx1
621 target genes [16]. Our TaDa datasets strongly point towards another function for
622 Fuss in *Drosophila*, as neither *hedgehog* nor the homologues of *Lbx1*, *ladybird late*
623 and *ladybird early*, are enriched in Fuss expressing cells. Therefore, identifying target
624 genes, interacting proteins, binding motifs of the Fuss complex and subsequent
625 comparison with established models for other transcription factor complexes will
626 elucidate the role of this complex in cell fate determination.

627

628 Material and Methods

629 *Drosophila* genetics

630 Flies were kept under standard conditions (25 °C, 12 h/12 h LD cycle). Flies from
631 RNA interference crosses were kept at 29 °C. Fly lines obtained from the
632 Bloomington Stock Center were *fuss*^{Mi13731} (#60860), UAS-*CD8-GFP* (#5137), UAS-
633 *CD8-RFP* (#32218), UAS-*LacZ* (#8529), *tubulin*-Gal80ts (#7108), UAS-*Stinger*

bioRxiv preprint doi: https://doi.org/10.1101/481721; this version posted November 29, 2018. The copyright holder for this preprint (which was not certified by peer review) is the author/funder, who has granted bioRxiv a license to display the preprint in perpetuity. It is made available under aCC-BY-ND 4.0 International license.

634 (#65402), UAS-*rpd3*-IR (#33725), UAS-*cherry*-IR (#35785), *ap*-Gal4 (#3041), *Gr33a*-
635 Gal4(#31425), *Gr66a*-Gal4 (#57670), *Gr93a*-Gal4 (#57679), *Hb9*-Gal4 (#32555),
636 *Gr5a*-Gal4 (#57591), *Ir76b*-Gal4 (#51311), UAS-*cas9* (#58985) and *ato*-Gal4
637 (#6480). UAS-*Dam* and UAS-*Dam-PolII* stocks were a gift from Andrea Brand. *Poxn*-
638 Gal4-13-1 was a gift from Markus Noll. UAS-*fussB*, *ap*-tau-LacZ and UAS-*rpr* were
639 from our stock collection. To generate the *fuss*^{delDS} line two sgRNAs
640 (GTAAGCTCCGTTTTGCTGTA and GGTGTTCCCTTTAACTTACA) were employed
641 and cloned into *pU6-BbsI-chiRNA*. Homology arms were cloned into *pHD-DsRed-*
642 *attP* and coinjected with *pU6-BbsI-chiRNA* as described in Gratz et al. [52]. The
643 *fussBD*-Gal4 and the *fuss*$^{Mi\text{-}cherry}$ lines were created via RMCE with the vectors *pBS-*
644 *KS-attB1-2-GT-SA-GAL4-Hsp70pA* and *pBS-KS-attB1-2-GT-SA-mCherry-SV40,*
645 *respectively* [27]. To generate the mutant *fuss*^{delDS}-Gal4 line, the *fussBD*-Gal4 line
646 was additionally targeted with the same sgRNAs via CRISPR/Cas9, which were used
647 for the *fuss*^{delDS} line. Genomic DNA of CantonS and *fuss*^{delDS} flies was extracted with
648 QIAamp DNA Mini Kit (Qiagen, Hilden, Germany). Successful indel mutation was
649 confirmed by PCR with Cr1seqfw (CAAATCGACTGGGTAAATGGT) and Cr2seqrv
650 (GTAGTCCACTACAAAGTTCCTG) oligonucleotides und subsequently sequenced
651 (GATC Biotech, Konstanz, Germany). *hs-fussB-GFP* was generated by cloning the
652 ORF of *fussB-GFP* into *pCaSpeR. hs-fussB-GFP* flies were generated via P-element
653 integration of *pCaSpeR-hs-fussB-GFP* vector into *w; +/Δ2-3, Ki* and subsequent
654 crossed to W^{1118} flies and transformants were balanced. For generation of UAS-
655 *t::gRNA-fuss*^{4x} flies we followed the protocol from Port et al. [28] and used primers,
656 which allow the targeting of the CRISPR target sites
657 GTAAGCTCCGTTTTGCTGTACGG, ATTGTATCCCTGCACATTGAAGG,
658 CCAGTGAGTTCCCGACGATGTGG and TTGAAATTTGCGCCAAGCAAAGG. The
659 *pCFD6-t::gRNA-fuss*^{4x} was injected into *y[1],M{vas-int.Dm}ZH-2A,w[*]; M{3xP3-*

bioRxiv preprint doi: https://doi.org/10.1101/481721; this version posted November 29, 2018. The copyright holder for this preprint (which was not certified by peer review) is the author/funder, who has granted bioRxiv a license to display the preprint in perpetuity. It is made available under aCC-BY-ND 4.0 International license.

660 *RFP.attP}ZH-86Fb* flies to generate UAS-*t::gRNA-fuss*^{4x} flies. All *Drosophila* strains
661 generated in this publication are available upon request.

662 **Polyclonal anti-Fuss antibody generation**

663 Fulllength *fuss* ORF was codon optimized at GeneArt, Regensburg, Germany. An
664 appropriate fragment of the codon optimized fuss gene was cloned into pQE60
665 resulting in a 16 kDa 6xHis tagged Fuss fragment called Fuss16-6xHis (Fig S1).
666 Transformed Rosetta2 cells were grown to an OD 0.6 and protein expression was
667 induced with 0.5 mM IPTG. Cells were incubated for 2.5 h at 37 °C, harvested,
668 resuspended in PBS supplemented with Protein Inhibitors (Roche, Switzerland) and
669 lysed via sonication. Fuss16-6xHis was purified with an Äktapurifier10 (GE
670 Healthcare, Life sciences) and was used for immunization of two rabbits at Davids
671 Biotechnologie, Regensburg, Germany. The resulting antiserum was purified against
672 Fuss16-6xHis to reduce nonspecific binding. Before using the anti-Fuss antibodies
673 for immunostainings or western blots they were preabsorbed using 0-6 h embryos
674 treated with 4 % PFA in PBST 0.1 % as follows: The antibody was diluted to 1:50 in
675 500ml PBST 0.1 %, NGS 5 % and incubated with 100 µl fixed embryos on a rotator
676 at 4 °C over night. Anti-Fuss antibody was further diluted to 1:200 in PBST 0.1 %,
677 NGS 5 % for immunostainings and 1:1000 in TBST 0.1 % for western blots.

678 **Real time PCR**

679 Sixty proboscises from each genotype (equal number of males and females) per
680 biological replicate were dissected on ice and snap-frozen in liquid nitrogen. RNA
681 was extracted by adding lysis buffer from the MicroSpin Total RNA Kit (VWR) and the
682 tissue was extracted with a bead mill and it was proceeded according to the
683 manufacturer’s protocol. cDNA was generated with the QuantiTect® Reverse
684 Transcription Kit (QIAGEN). For subsequent real time PCR ORA qPCR Green ROX L

bioRxiv preprint doi: https://doi.org/10.1101/481721; this version posted November 29, 2018. The copyright holder for this preprint (which was not certified by peer review) is the author/funder, who has granted bioRxiv a license to display the preprint in perpetuity. It is made available under aCC-BY-ND 4.0 International license.

685 Mix (HighQu, Kralchtal, Germany) was employed. RP49 was used as a housekeeper
686 control, with the primers RP49fw (CCAAGCACTTCATCCGCCACC) and RP49rv
687 (GCGGGTGCGCTTGTTCGATCC). Primer sequences for Gr33afw
688 (CCACCATCGCGGAAAATAC), Gr33arv (ACACACTGTGGTCCAAACTC), Gr66afw
689 (ACAGGAATCAGTCTGCACAA), Gr66arv (AATGTTTCCATGTCCAGGGT), Gr93afw
690 (CCACGTCACAAACTCATTCC), Gr93rv (GCCATCACAATGGACACAAA), fussBDfw
691 (TGGCTTCTATATCTGTGGCTCA) and fussBDrv (CAAAGGCGCTCTTGACCTTC)
692 were generated with PrimerBlast. For relative quantification, we applied the ΔΔCT
693 method. Every experiment has been repeated at least four times.

694 **Protein expression analysis**

695 Developmental studies Hybridoma Bank (DSHB) antibodies were: Acj6 (1:50), Dac
696 (Mabdac1-1, 1:20), EcRB1 (AD4.4, 1:50), LacZ (JIE7, 1:20), Pros (MR1A, 1:10), Elav
697 (7E8A10, 1:50), Engrailed (4D9, 1:20), Even skipped (3C10, 1:20) Repo (8D12,
698 1:20), and Fas2 (1D4 1:10). Additional antibodies were: Pale (AB152, 1:500,
699 Millipore), Ilp2 (1:400, gift from Pierre Leopold), Toy (1:200, gift from U. Walldorf),
700 GFP (goat 1:100, Rockland; rabbit 1:1000, ThermoFisher), RFP (rabbit 1:20,
701 ThermoFisher) and anti-phospho-SMAD1/5 (1:50, Cell signaling). Secondary
702 antibodies were goat anti-mouse, anti-rabbit, anti-rat and anti-guinea pig Alexa Fluor
703 488, 555 and 594 (ThermoFisher). Samples were analysed with a Leica SP8
704 microscope. To confirm functionality of anti-Fuss antibodies *hs-fussB-GFP* third instar
705 larvae were heatshocked for one hour at 37 °C and were allowed to recover for
706 another hour at room temperature. RIPA buffer was added to ten larvae and they
707 were mechanically disrupted. Insoluble fragments were removed by centrifugation
708 and supernatant was incubated at 95 °C for five minutes. Supernatant was analysed
709 via SDS-Page and Western blotting. As a housekeeper mouse anti-tubulin (B-5-1-2,
710 MERCK) was utilised and secondary antibodies were goat anti-mouse 680nm and

bioRxiv preprint doi: https://doi.org/10.1101/481721; this version posted November 29, 2018. The copyright holder for this preprint (which was not certified by peer review) is the author/funder, who has granted bioRxiv a license to display the preprint in perpetuity. It is made available under aCC-BY-ND 4.0 International license.

711 goat anti-rabbit 800nm (Li-Cor, Lincoln, USA). Signals were detected using an
712 Odyssey infrared imaging system (Li-Cor, Lincoln, USA).

713 **Co-Immunoprecipitation**

714 S2R+ cells were cultured in Schneider's *Drosophila* Medium (Pan Biotech,
715 Aidenbach, Germany) supplemented with 10 % Fetal Bovine Serum (Pan Biotech,
716 Aidenbach, Germany). The coding regions of *fussB, smox* and *rpd3* were inserted
717 into pFSR11.58 3xHA and pFSR12.51 4xFlag (Frank Sprenger, Regensburg,
718 Germany). Cells were transfected in 6 well plates at 70 % confluency with 2 µg of
719 pFSR11.58 Fuss-HA and pFSR12.51 Rpd3-Flag (or Smox-Flag), or pFSR11.58
720 RPD3-HA (or Smox-HA) and pFSR12.51 Fuss-Flag, respectively, using
721 Lipofectamine 3000 (Thermo Scientific, Waltham, MA, USA) according to the
722 manufacturer's protocol and incubated for another 24 h. Transfected cells were
723 harvested using a plastic scraper. For Rpd3 and Fuss interaction experiments
724 nuclear extracts were prepared using the NE-PER Nuclear and Cytoplasmic
725 Extraction Reagents (Thermo Scientific, Waltham, MA, USA) and only nuclear
726 fraction was used. For Fuss and Smox interaction whole cell extracts were prepared
727 with 400 µl lysis buffer (50 mM HEPES pH 7.5, 150 mM NaCl 150, 1 % Triton X-100,
728 10% Glycerol, 1 mM EGTA, 10 mM NaF) supplemented with cOmplete™ Mini
729 Protease Inhibitor Cocktail (Roche, Switzerland). After preclearing the extracts with
730 30 µl Protein A-Agarose beads (Santa Cruz, Dallas, TX, USA) and conjugating 1.5 µl
731 Anti-Flag M2 antibody (Sigma, St. Luis, Mo, USA) to 30 µl Protein A/G Plus beads
732 (Santa Cruz, Dallas, TX, USA), the volume of the nuclear extract was brought up to
733 400 µl using RIPA buffer (50 mM Tris (pH 7.5), 150 mM NaCl, 1 % (v/v) NP-40, 0.5 %
734 (w/v) Deoxycholat) supplemented with cOmplete™ Mini Protease Inhibitor Cocktail
735 (Roche, Switzerland). 5% of the precleared extracts were saved for input analysis.
736 Immunoprecipitation was conducted for 2 h at 4 °C. Following three washing steps

bioRxiv preprint doi: https://doi.org/10.1101/481721; this version posted November 29, 2018. The copyright holder for this preprint (which was not certified by peer review) is the author/funder, who has granted bioRxiv a license to display the preprint in perpetuity. It is made available under aCC-BY-ND 4.0 International license.

737 with RIPA buffer, the precipitated proteins, as well as the precleared nuclear extracts,
738 were analyzed by SDS-PAGE and western blotting. As primary antibodies Anti-Flag
739 M2 and Anti-HA.11 (Covance Inc. USA) were used. Secondary antibody was goat
740 anti mouse 680 (Li-Cor). Signals were detected using an Odyssey infrared imaging
741 system (Li-Cor, Lincoln, USA).

742 **Targeted DamID and Bioinformatics**

743 Targeted DamID to profile transcription in Fuss expressing neurons was performed
744 as previously described [34,65,66]. UAS-*Dam,* UAS-*DamPolII,* UAS-*Dam; fuss*^{delDS} *or*
745 UAS-*DamPolII; fuss*^{delDS} flies were crossed to *tubulin*-Gal80^{ts}*; fuss*^{delDS}-Gal4 flies.
746 Three biological replicates of *DamPolII* expressing flies and three biological replicates
747 of Dam expressing flies were conducted. Per replicate 100 one to three-day old flies
748 (50 females and 50 males) were incubated for 24 h at 29 °C and snap-frozen in liquid
749 nitrogen. Heads were detached by vortexing and separated with sieves. Processing
750 of genomic DNA from heads and data analysis were performed as described and
751 NGS libraries libraries were prepared with NEBNext UltraII DNA Library Prep Kit for
752 Illumina [34,65,66]. Sequencing was carried out by the Biomedical Sequencing
753 Facility at CeMM. For aligning reads, dm6 release from UCSC was used. Data tracks
754 from same genotype were averaged with the average_tracks script and 3150 genes
755 were called with an FDR < 0.01 for mutant flies and 2932 genes for control flies.
756 log2(Dam-PolII/Dam) ratio datasets were visualized with the Integrative Genomic
757 Browser.

758 **Life span**

759 For life span determination, male flies were collected within 24 h after eclosion and
760 were raised at 25 °C under a 12 h:12 h light/dark cycle. These flies were transferred
761 to fresh food vials every two to three days.

bioRxiv preprint doi: https://doi.org/10.1101/481721; this version posted November 29, 2018. The copyright holder for this preprint (which was not certified by peer review) is the author/funder, who has granted bioRxiv a license to display the preprint in perpetuity. It is made available under aCC-BY-ND 4.0 International license.

762 **Two choice feeding assay**

763 Feeding behaviour was analysed as previously described at 25 °C [38]. Fly age at
764 time of testing ranged from one to three days and experiments were only accounted if
765 at least 30 % of all flies showed clear evaluable coloured abdomen. As bitter
766 compounds caffeine and denatonium benzoate were utilised at the indicated
767 concentrations. Because feeding behaviour was influenced by temperature, *fussBD*-
768 Gal4 x UAS-*cherry*-IR and *fussBD*-Gal4 x UAS-*rpd3*-IR flies were shifted to 25°C two
769 hours prior testing. Every experiment has been repeated at least four times.

770 **Preparation of Figures**

771 All figures were assembled with Adobe Photoshop CC (Adobe Systems) by importing
772 microscopy images from Fiji and graphs from Prism.

773 **Statistics**

774 Survival data were analyzed using the Log-rank (Mantel-Cox) and Gehan-Breslow-
775 Wilcoxon tests. Significance was determined by two-tailed t-test or by One-way
776 ANOVA with *post hoc* Tukey Multiple Comparison Test (****p<0.001; ***p<0.001;
777 **p<0.01 and *p<0.05). Statistical analysis was carried out using Prism version 7.0a
778 for MacOs, GraphPad Software, La Jolla, CA, USA.

779 **Availability**

780 Raw sequencing data are accessible via Gene Expression Omnibus: GEO Series
781 GSE115347.

782 Acknowledgements

783 We thank Juan A. Navarro for critically reading the manuscript. We thank Renate
784 Reng for technical assistance. We thank Lars Kullmann as well as Caroline Iglhaut
785 for the generation of *HS-FussB-GFP* flies and Matthias Schramm for the generation

bioRxiv preprint doi: https://doi.org/10.1101/481721; this version posted November 29, 2018. The copyright holder for this preprint (which was not certified by peer review) is the author/funder, who has granted bioRxiv a license to display the preprint in perpetuity. It is made available under aCC-BY-ND 4.0 International license.

786 of the appropriate vectors for the *fuss*^{delDS} flies. We thank Frank Sprenger for
787 providing pFSR vectors, Markus Noll for *Poxn*-Gal4-13-1 flies and Andrea H. Brand
788 for UAS-*Dam* and UAS-*Dam-PolII* vectors and flies. We thank Michael Rehli and
789 Owen J. Marshall for support regarding NGS library preparation and bioinformatical
790 analysis. We would like to thank the Biomedical Sequencing Facility at CeMM for
791 sequencing. Stocks obtained from the Bloomington Drosophila Stock Center (NIH
792 P40OD018537) and antibodies from Developmental Studies Hybridoma Bank were
793 used in this study.

794 **References**

795 1. Massagué J. TGF-beta signal transduction. Annu Rev Biochem. 1998; 67: 753–
796 791. doi: 10.1146/annurev.biochem.67.1.753.

797 2. Deheuninck J, Luo K. Ski and SnoN, potent negative regulators of TGF-beta
798 signaling. Cell Res. 2009; 19: 47–57. doi: 10.1038/cr.2008.324.

799 3. Ebisawa T, Fukuchi M, Murakami G, Chiba T, Tanaka K, Imamura T, et al.
800 Smurf1 interacts with transforming growth factor-beta type I receptor through
801 Smad7 and induces receptor degradation. J Biol Chem. 2001; 276: 12477–
802 12480. doi: 10.1074/jbc.C100008200.

803 4. Hayashi H, Abdollah S, Qiu Y, Cai J, Xu Y-Y, Grinnell BW, et al. The MAD-
804 Related Protein Smad7 Associates with the TGFβ Receptor and Functions as an
805 Antagonist of TGFβ Signaling. Cell. 1997; 89: 1165–1173. doi: 10.1016/S0092-
806 8674(00)80303-7.

807 5. Boone B, Haspeslagh M, Brochez L. Clinical significance of the expression of c-
808 Ski and SnoN, possible mediators in TGF-β resistance, in primary cutaneous
809 melanoma. Journal of Dermatological Science; 53: 26–33.
810 doi: 10.1016/j.jdermsci.2008.07.010.

811 6. Shinagawa T, Dong HD, Xu M, Maekawa T, Ishii S. The sno gene, which
812 encodes a component of the histone deacetylase complex, acts as a tumor
813 suppressor in mice. EMBO J. 2000; 19: 2280–2291.
814 doi: 10.1093/emboj/19.10.2280.

815 7. Jahchan NS, Wang D, Bissell MJ, Luo K. SnoN regulates mammary gland
816 alveologenesis and onset of lactation by promoting prolactin/Stat5 signaling.
817 Development. 2012; 139: 3147–3156. doi: 10.1242/dev.079616.

818 8. Berk M, Desai SY, Heyman HC, Colmenares C. Mice lacking the ski proto-
819 oncogene have defects in neurulation, craniofacial patterning, and skeletal

bioRxiv preprint doi: https://doi.org/10.1101/481721; this version posted November 29, 2018. The copyright holder for this preprint (which was not certified by peer review) is the author/funder, who has granted bioRxiv a license to display the preprint in perpetuity. It is made available under aCC-BY-ND 4.0 International license.

820 muscle development. Genes & Development. 1997; 11: 2029–2039.
821 doi: 10.1101/gad.11.16.2029.

822 9. Stegmüller J, Konishi Y, Huynh MA, Yuan Z, DiBacco S, Bonni A. Cell-Intrinsic
823 Regulation of Axonal Morphogenesis by the Cdh1-APC Target SnoN. Neuron.
824 2006; 50: 389–400. doi: 10.1016/j.neuron.2006.03.034.

825 10. Nomura T, Khan MM, Kaul SC, Dong H-D, Wadhwa R, Colmenares C, et al. Ski
826 is a component of the histone deacetylase complex required for transcriptional
827 repression by Mad and thyroid hormone receptor. Genes & Development. 1999;
828 13: 412–423.

829 11. Wu J-W, Krawitz AR, Chai J, Li W, Zhang F, Luo K, et al. Structural Mechanism
830 of Smad4 Recognition by the Nuclear Oncoprotein Ski: Insights on Ski-Mediated
831 Repression of TGF-β Signaling. Cell. 2002; 111: 357–367. doi: 10.1016/S0092-
832 8674(02)01006-1.

833 12. Wilson JJ, Malakhova M, Zhang R, Joachimiak A, Hegde RS. Crystal Structure
834 of the Dachshund Homology Domain of Human SKI. Structure; 12: 785–792.
835 doi: 10.1016/j.str.2004.02.035.

836 13. Arndt S, Poser I, Moser M, Bosserhoff A-K. Fussel-15, a novel Ski/Sno homolog
837 protein, antagonizes BMP signaling. Molecular and Cellular Neuroscience. 2007;
838 34: 603–611. doi: 10.1016/j.mcn.2007.01.002.

839 14. Arndt S, Poser I, Schubert T, Moser M, Bosserhoff A-K. Cloning and functional
840 characterization of a new Ski homolog, Fussel-18, specifically expressed in
841 neuronal tissues. Lab Invest. 2005; 85: 1330–1341.
842 doi: 10.1038/labinvest.3700344.

843 15. Nakatani T, Minaki Y, Kumai M, Nitta C, Ono Y. The c-Ski family member and
844 transcriptional regulator Corl2/Skor2 promotes early differentiation of cerebellar
845 Purkinje cells. Developmental Biology. 2014; 388: 68–80.
846 doi: 10.1016/j.ydbio.2014.01.016.

847 16. Mizuhara E, Nakatani T, Minaki Y, Sakamoto Y, Ono Y. Corl1, a novel neuronal
848 lineage-specific transcriptional corepressor for the homeodomain transcription
849 factor Lbx1. J Biol Chem. 2005; 280: 3645–3655. doi: 10.1074/jbc.M411652200.

850 17. Wang B, Harrison W, Overbeek PA, Zheng H. Transposon mutagenesis with
851 coat color genotyping identifies an essential role for Skor2 in sonic hedgehog
852 signaling and cerebellum development. Development. 2011; 138: 4487–4497.
853 doi: 10.1242/dev.067264.

854 18. Fischer S, Bayersdorfer F, Harant E, Reng R, Arndt S, Bosserhoff A-K, et al.
855 fussel (fuss) - A Negative Regulator of BMP Signaling in Drosophila
856 melanogaster. PLOS ONE. 2012; 7: 1–12. doi: 10.1371/journal.pone.0042349.

857 19. Barrio R, López-Varea A, Casado M, de Celis JF. Characterization of dSnoN and
858 its relationship to Decapentaplegic signaling in Drosophila. Developmental
859 Biology. 2007; 306: 66–81. doi: 10.1016/j.ydbio.2007.02.039.

bioRxiv preprint doi: https://doi.org/10.1101/481721; this version posted November 29, 2018. The copyright holder for this preprint (which was not certified by peer review) is the author/funder, who has granted bioRxiv a license to display the preprint in perpetuity. It is made available under aCC-BY-ND 4.0 International license.

860 20. Djabrayan NJ-V, Casanova J. Snoo and Dpp Act as Spatial and Temporal
861 Regulators Respectively of Adult Progenitor Cells in the Drosophila Trachea.
862 PLOS Genetics. 2016; 12: 1–15. doi: 10.1371/journal.pgen.1005909.

863 21. Shravage BV, Altmann G, Technau M, Roth S. The role of Dpp and its inhibitors
864 during eggshell patterning in Drosophila. Development. 2007; 134: 2261–2271.
865 doi: 10.1242/dev.02856.

866 22. Takaesu NT, Stinchfield MJ, Shimizu K, Arase M, Quijano JC, Watabe T, et al.
867 Drosophila CORL is required for Smad2-mediated activation of Ecdysone
868 Receptor expression in the mushroom body. Development. 2012; 139: 3392–
869 3401. doi: 10.1242/dev.079442.

870 23. Zhang X, Koolhaas WH, Schnorrer F. A versatile two-step CRISPR- and RMCE-
871 based strategy for efficient genome engineering in Drosophila. G3 (Bethesda,
872 Md.). 2014; 4: 2409–2418. doi: 10.1534/g3.114.013979.

873 24. Blanco J, Pauli T, Seimiya M, Udolph G, Gehring WJ. Genetic interactions of
874 eyes absent, twin of eyeless and orthodenticle regulate sine oculis expression
875 during ocellar development in Drosophila. Developmental Biology. 2010; 344:
876 1088–1099. doi: 10.1016/j.ydbio.2010.05.494.

877 25. Ueki N, Hayman MJ. Signal-dependent N-CoR requirement for repression by the
878 Ski oncoprotein. J Biol Chem. 2003; 278: 24858–24864.
879 doi: 10.1074/jbc.M303447200.

880 26. Luo K, Stroschein SL, Wang W, Chen D, Martens E, Zhou S, et al. The Ski
881 oncoprotein interacts with the Smad proteins to repress TGFβ signaling. Genes
882 & Development. 1999; 13: 2196–2206.

883 27. Venken KJT, Schulze KL, Haelterman NA, Pan H, He Y, Evans-Holm M, et al.
884 MiMIC: a highly versatile transposon insertion resource for engineering
885 Drosophila melanogaster genes. Nature methods. 2011; 8: 737–743.

886 28. Port F, Bullock SL. Augmenting CRISPR applications in Drosophila with tRNA-
887 flanked Cas9 and Cpf1 sgRNAs. Nature methods. 2016; 13: 852–854.
888 doi: 10.1038/nmeth.3972.

889 29. Broihier HT, Skeath JB. Drosophila Homeodomain Protein dHb9 Directs
890 Neuronal Fate via Crossrepressive and Cell-Nonautonomous Mechanisms.
891 Neuron; 35: 39–50. doi: 10.1016/S0896-6273(02)00743-2.

892 30. Landgraf M, Roy S, Prokop A, VijayRaghavan K, Bate M. even-skipped
893 Determines the Dorsal Growth of Motor Axons in Drosophila. Neuron. 1999; 22:
894 43–52. doi: 10.1016/S0896-6273(00)80677-7.

895 31. Hammond KL, Hanson IM, Brown AG, Lettice LA, Hill RE. Mammalian and
896 Drosophila dachshund genes are related to the Ski proto-oncogene and are
897 expressed in eye and limb. Mechanisms of Development. 1998; 74: 121–131.
898 doi: 10.1016/S0925-4773(98)00071-9.

bioRxiv preprint doi: https://doi.org/10.1101/481721; this version posted November 29, 2018. The copyright holder for this preprint (which was not certified by peer review) is the author/funder, who has granted bioRxiv a license to display the preprint in perpetuity. It is made available under aCC-BY-ND 4.0 International license.

899 32. Miguel-Aliaga I, Allan DW, Thor S. Independent roles of the dachshund and eyes
900 absent genes in BMP signaling, axon pathfinding and neuronal specification.
901 Development. 2004; 131: 5837–5848. doi: 10.1242/dev.01447.

902 33. Lundgren SE, Callahan CA, Thor S, Thomas JB. Control of neuronal pathway
903 selection by the Drosophila LIM homeodomain gene apterous. Development.
904 1995; 121: 1769–1773.

905 34. Southall TD, Gold KS, Egger B, Davidson CM, Caygill EE, Marshall OJ, et al.
906 Cell-Type-Specific Profiling of Gene Expression and Chromatin Binding without
907 Cell Isolation: Assaying RNA Pol II Occupancy in Neural Stem Cells.
908 Developmental Cell. 2013; 26: 101–112. doi: 10.1016/j.devcel.2013.05.020.

909 35. Tran NL, Takaesu NT, Cornell EF, Newfeld SJ. CORL Expression in the
910 Drosophila Central Nervous System Is Regulated by Stage Specific Interactions
911 of Intertwined Activators and Repressors. G3 (Bethesda, Md.). 2018.
912 doi: 10.1534/g3.118.200282.

913 36. Tran NL, Goldsmith SL, Dimitriadou A, Takaesu NT, Consoulas C, Newfeld SJ.
914 CORL Expression and Function in Insulin Producing Neurons Reversibly
915 Influences Adult Longevity in Drosophila. G3 (Bethesda, Md.). 2018; 8: 2979–
916 2990. doi: 10.1534/g3.118.200572.

917 37. Besson M.T., Sinakevitch I., Melon C., Iché-Torres M., Birman S. Involvement of
918 the drosophila taurine/aspartate transporter dEAAT2 in selective olfactory and
919 gustatory perceptions. J. Comp. Neurol. 2011; 519: 2734–2757.
920 doi: 10.1002/cne.22649.

921 38. Moon SJ, Köttgen M, Jiao Y, Xu H, Montell C. A Taste Receptor Required for the
922 Caffeine Response In Vivo. Current Biology; 16: 1812–1817.
923 doi: 10.1016/j.cub.2006.07.024.

924 39. Ahn J-E, Chen Y, Amrein H. Molecular basis of fatty acid taste inDrosophila.
925 Elife. 2017; 6. doi: 10.7554/eLife.30115.

926 40. Moon SJ, Lee Y, Jiao Y, Montell C. A Drosophila Gustatory Receptor Essential
927 for Aversive Taste and Inhibiting Male-to-Male Courtship. Current Biology; 19:
928 1623–1627. doi: 10.1016/j.cub.2009.07.061.

929 41. Apostolopoulou AA, Köhn S, Stehle B, Lutz M, Wüst A, Mazija L, et al. Caffeine
930 Taste Signaling in Drosophila Larvae. Frontiers in Cellular Neuroscience. 2016;
931 10: 193. doi: 10.3389/fncel.2016.00193.

932 42. Choi J, van Giesen L, Choi MS, Kang K, Sprecher SG, Kwon JY. A Pair of
933 Pharyngeal Gustatory Receptor Neurons Regulates Caffeine-Dependent
934 Ingestion in Drosophila Larvae. Frontiers in Cellular Neuroscience. 2016; 10:
935 1523. doi: 10.3389/fncel.2016.00181.

936 43. Amrein H, Thorne N. Gustatory Perception and Behavior in Drosophila
937 melanogaster. Current Biology. 2005; 15: R673-R684.
938 doi: 10.1016/j.cub.2005.08.021.

bioRxiv preprint doi: https://doi.org/10.1101/481721; this version posted November 29, 2018. The copyright holder for this preprint (which was not certified by peer review) is the author/funder, who has granted bioRxiv a license to display the preprint in perpetuity. It is made available under aCC-BY-ND 4.0 International license.

939 44. Zhang YV, Ni J, Montell C. The molecular basis for attractive salt-taste coding in
940 Drosophila. Science. 2013; 340: 1334–1338. doi: 10.1126/science.1234133.

941 45. Freeman EG, Dahanukar A. Molecular neurobiology of Drosophila taste. Curr
942 Opin Neurobiol. 2015; 34: 140–148. doi: 10.1016/j.conb.2015.06.001.

943 46. Ebbs ML, Amrein H. Taste and pheromone perception in the fruit fly Drosophila
944 melanogaster. Pflugers Arch. 2007; 454: 735–747. doi: 10.1007/s00424-007-
945 0246-y.

946 47. Boll W, Noll M. The Drosophila Pox neuro gene: control of male courtship
947 behavior and fertility as revealed by a complete dissection of all enhancers.
948 Development. 2002; 129: 5667–5681. doi: 10.1242/dev.00157.

949 48. Lee Y, Moon SJ, Montell C. Multiple gustatory receptors required for the caffeine
950 response in Drosophila. Proceedings of the National Academy of Sciences.
951 2009; 106: 4495–4500. doi: 10.1073/pnas.0811744106.

952 49. Bosch PS, Ziukaite R, Alexandre C, Basler K, Vincent J-P. Dpp controls growth
953 and patterning in Drosophila wing precursors through distinct modes of action.
954 Elife. 2017; 6: 375. doi: 10.7554/eLife.22546.

955 50. Allan DW, Pierre SES, Miguel-Aliaga I, Thor S. Specification of Neuropeptide
956 Cell Identity by the Integration of Retrograde BMP Signaling and a Combinatorial
957 Transcription Factor Code. Cell. 2003; 113: 73–86. doi: 10.1016/S0092-
958 8674(03)00204-6.

959 51. Marqués G, Bao H, Haerry TE, Shimell MJ, Duchek P, Zhang B, et al. The
960 Drosophila BMP Type II Receptor Wishful Thinking Regulates Neuromuscular
961 Synapse Morphology and Function. Neuron. 2002; 33: 529–543.
962 doi: 10.1016/S0896-6273(02)00595-0.

963 52. Gratz SJ, Ukken FP, Rubinstein CD, Thiede G, Donohue LK, Cummings AM, et
964 al. Highly specific and efficient CRISPR/Cas9-catalyzed homology-directed
965 repair in Drosophila. Genetics. 2014; 196: 961–971.
966 doi: 10.1534/genetics.113.160713.

967 53. Shim J, Lee Y, Jeong YT, Kim Y, Lee MG, Montell C, et al. The full repertoire of
968 Drosophila gustatory receptors for detecting an aversive compound. Nat
969 Commun. 2015; 6. doi: 10.1038/ncomms9867.

970 54. Poudel S, Lee Y. Gustatory Receptors Required for Avoiding the Toxic
971 Compound Coumarin in Drosophila melanogaster. Mol Cells. 2016; 39: 310–315.
972 doi: 10.14348/molcells.2016.2250.

973 55. Huang M-L, Hsu C-H, Chien C-T. The Proneural Gene amos Promotes Multiple
974 Dendritic Neuron Formation in the Drosophila Peripheral Nervous System.
975 Neuron. 2000; 25: 57–67. doi: 10.1016/S0896-6273(00)80871-5.

976 56. Jarman AP, Grau Y, Jan LY, Jan YN. atonal is a proneural gene that directs
977 chordotonal organ formation in the Drosophila peripheral nervous system. Cell.
978 1993; 73: 1307–1321. doi: 10.1016/0092-8674(93)90358-W.

bioRxiv preprint doi: https://doi.org/10.1101/481721; this version posted November 29, 2018. The copyright holder for this preprint (which was not certified by peer review) is the author/funder, who has granted bioRxiv a license to display the preprint in perpetuity. It is made available under aCC-BY-ND 4.0 International license.

979 57. Nolo R, Abbott LA, Bellen HJ. Senseless, a Zn Finger Transcription Factor, Is
980 Necessary and Sufficient for Sensory Organ Development in Drosophila. Cell.
981 2000; 102: 349–362. doi: 10.1016/S0092-8674(00)00040-4.

982 58. Chen G, Fernandez J, Mische S, Courey AJ. A functional interaction between the
983 histone deacetylase Rpd3 and the corepressor Groucho in Drosophila
984 development. Genes & Development. 1999; 13: 2218–2230.

985 59. Furukubo-Tokunaga K, Adachi Y, Kurusu M, Walldorf U. Brain patterning defects
986 caused by mutations of the twin of eyeless gene in Drosophila melanogaster. Fly.
987 2009; 3: 263–269. doi: 10.4161/fly.10385.

988 60. Akiyoshi S, Inoue H, Hanai J-i, Kusanagi K, Nemoto N, Miyazono K, et al. c-Ski
989 Acts as a Transcriptional Co-repressor in Transforming Growth Factor-β
990 Signaling through Interaction with Smads. J Biol Chem. 1999; 274: 35269–
991 35277. doi: 10.1074/jbc.274.49.35269.

992 61. Sun Y, Liu X, Eaton EN, Lane WS, Lodish HF, Weinberg RA. Interaction of the
993 Ski Oncoprotein with Smad3 Regulates TGF-β Signaling. Molecular Cell. 1999;
994 4: 499–509. doi: 10.1016/S1097-2765(00)80201-4.

995 62. Das P, Inoue H, Baker JC, Beppu H, Kawabata M, Harland RM, et al. Drosophila
996 dSmad2 and Atr-I transmit activin/TGFbeta signals. Genes Cells. 1999; 4: 123–
997 134. doi: 10.1046/j.1365-2443.1999.00244.x.

998 63. Nyman T, Trésaugues L, Welin M, Lehtiö L, Flodin S, Persson C, et al. The
999 Crystal Structure of the Dachshund Domain of Human SnoN Reveals Flexibility
1000 in the Putative Protein Interaction Surface. PLOS ONE. 2010; 5: e12907.
1001 doi: 10.1371/journal.pone.0012907.

1002 64. Tecalco-Cruz AC, Ríos-López DG, Vázquez-Victorio G, Rosales-Alvarez RE,
1003 Macías-Silva M. Transcriptional cofactors Ski and SnoN are major regulators of
1004 the TGF-β/Smad signaling pathway in health and disease. Signal Transduction
1005 and Targeted Therapy. 2018; 3: 15. doi: 10.1038/s41392-018-0015-8.

1006 65. Marshall OJ, Brand AH. damidseq_pipeline: an automated pipeline for
1007 processing DamID sequencing datasets. Bioinformatics. 2015; 31: 3371–3373.
1008 doi: 10.1093/bioinformatics/btv386.

1009 66. Marshall OJ, Southall TD, Cheetham SW, Brand AH. Cell-type-specific profiling
1010 of protein-DNA interactions without cell isolation using targeted DamID with next-
1011 generation sequencing. Nat Protoc. 2016; 11: 1586–1598.
1012 doi: 10.1038/nprot.2016.084.

1013

1014 Figure legends

1015 **Fig 1. Generation of CRISPR/Cas9 induced *fuss* mutant.** (A) Generation of a *fuss*
1016 knockout allele, which lacks the Ski/Sno/Dac homology domain (blue box) and the

bioRxiv preprint doi: https://doi.org/10.1101/481721; this version posted November 29, 2018. The copyright holder for this preprint (which was not certified by peer review) is the author/funder, who has granted bioRxiv a license to display the preprint in perpetuity. It is made available under aCC-BY-ND 4.0 International license.

1017 SMAD4 binding domain (yellow box) by means of two CRISPR target sites Cr1 and
1018 Cr2. The location of the second mutant allele *fuss*^{Mi13731}, a gene trap insertion in the
1019 FussB and FussD transcript is indicated. Approximate locations of *toy*, *sphinx* and
1020 *cr44030* are depicted as black arrows. The location of the transposable element *Tc1-*
1021 *2* is shown as a double-sided arrow. (B) Differences in the mean lifespan of
1022 homozygous *fuss*^{delDS} flies (n=133, purple) and the two controls W^{1118} (n=116, black)
1023 and *fuss*^{delDS} x W^{1118} flies (n=109, blue) are not relevant. C) Longevity experiments
1024 show no differences between homozygous *fuss*^{Mi13731} (n=164, purple), heterozygous
1025 *fuss*^{Mi13731} x WTB (n=136, blue) and WTB flies (n=85, black). (D) Projection pattern
1026 and cell bodies of larval brains visualized by expression of UAS-*CD8-GFP* by
1027 *fuss*^{delDS}-Gal4/+ larvae (control). (E) Projection pattern and cell bodies of larval brains
1028 visualized by expression of UAS-*CD8-GFP* by *fuss* mutant *fuss*^{delDS}-Gal4/*fuss*^{delDS}
1029 larvae (mutant). (F) Projection pattern and cell bodies of adult brains visualized by
1030 expression of UAS-*CD8-GFP* by *fuss*^{delDS}-Gal4/+ flies (control). (G) Projection pattern
1031 and cell bodies of adult brains visualized by expression of UAS-*CD8-GFP* by *fuss*
1032 mutant *fuss*^{delDS}-Gal4/*fuss*^{delDS} flies (mutant). Scale bars indicate 50 µm.

1033 **Fig 2. Fuss is expressed in postmitotic interneurons.** (A) In stage 16 embryos,
1034 anti-Fuss staining can be observed in a restricted number of cells in the CNS
1035 (dashed circles). Fuss is also found in individual cells of the stomatogastric nervous
1036 system (arrowhead) and anterior to the CNS (arrows). (B) In the ventral nerve cord
1037 (VNC), Fuss is expressed in two to five neurons per hemineuromer in ascending
1038 number from posterior to anterior. (C) Confocal microscopy images reveal that Fuss
1039 expressing cells in the VNC (green) do not overlap with ganglion mother cells stained
1040 with anti-Prospero (red). (D) Fuss is exclusively expressed in neurons (Elav, red) but
1041 not in glia (Repo, blue). (E, F) In one representative hemineuromer five Fuss (green)
1042 positive neurons are characterized regarding their Dac (blue, arrowhead) or Toy (red,

bioRxiv preprint doi: https://doi.org/10.1101/481721; this version posted November 29, 2018. The copyright holder for this preprint (which was not certified by peer review) is the author/funder, who has granted bioRxiv a license to display the preprint in perpetuity. It is made available under aCC-BY-ND 4.0 International license.

1043 arrow) expression. (G) In every hemineuromer one Fuss (green) neuron is positive
1044 for LacZ (red) expressed under the *apterous* promotor. Scale bars indicate 25µm (A),
1045 50µm (B), 10 µm (C, E, F) and 20 µm (D, G).

1046 **Fig 3. Targeted DamID of control and *fuss* mutants reveal sensory neuron**
1047 **markers as potential Fuss targets.** (A) A Dam-PolII/Dam binding pattern was
1048 generated from nine individual TaDa profiles and averaged to one single track. *fuss*
1049 (red box) and *toy* (blue box) are highly covered by Dam-PolII. Regions bound
1050 stronger by Dam-PolII than by Dam are depicted in green. Regions bound stronger
1051 by Dam than by Dam-PolII are depicted in red. (B) Verification of three TaDa positive
1052 genes, *toy*, *atonal* and *acj6* by immunostaining. Toy was labelled by anti-Toy (green)
1053 and Fuss by anti-Fuss staining (red). Expression of LacZ by *ato*-Gal4 (green) and
1054 expression of GFP from the $fuss^{Mi13731}$/+ reporter line (red). Labelling of Acj6 with
1055 anti-Acj6 antibody (green) and expression of CD8-GFP with *fussBD*-Gal4 (red). Scale
1056 bars indicate 10 µm. (C) log2(Dam-PolII/Dam) data from controls compared with
1057 log2(Dam-PolII/Dam) data from mutant Fuss neurons show only small deviations
1058 from each other. Coefficient of determination $R^2 = 0.889$. (D) TaDa reveals sensory
1059 neuron marker expression of *EAAT2*, *Ir76a*, and *Gr66a* in both datasets (upper lane:
1060 control; lower lane: mutant) with a clear reduction in PolII coverage of *Gr66a* in the
1061 mutant dataset in contrast to the control dataset. PolII coverage is depicted under
1062 PolII binding pattern. Regions bound stronger by Dam-PolII than by Dam are
1063 depicted in green. Regions bound stronger by Dam than by Dam-PolII are depicted in
1064 red.

1065 **Fig 4. Fuss is expressed in bitter GRNs in inner gustatory organs of larvae and**
1066 **in bitter and salt attracting GRNs of the adult proboscis.** (A) GFP (red)
1067 expression from heterozygous $fuss^{Mi13731}$/+ reporter line can be observed in bitter

bioRxiv preprint doi: https://doi.org/10.1101/481721; this version posted November 29, 2018. The copyright holder for this preprint (which was not certified by peer review) is the author/funder, who has granted bioRxiv a license to display the preprint in perpetuity. It is made available under aCC-BY-ND 4.0 International license.

1068 gustatory neurons marked with LacZ (green) expressed via *Gr33a*-Gal4 in the dorsal
1069 (DPS), posterior pharyngeal sensilia (PPS) and dorsal pharyngeal organ (DPO)
1070 identifying Fuss neurons as bitter gustatory neurons in these organs. (B) LacZ
1071 (green) expressed from a *Gr93a*-Gal4 line colocalizes with GFP (red) from a
1072 heterozygous $fuss^{Mi13731}$/+ reporter line. Scale bars indicate 10 µm. (C) In adult flies,
1073 GFP (red) expression from the $fuss^{Mi13731}$ gene trap line can be observed in the
1074 proboscis in one GRN per bristle. LacZ (green) driven by the bitter gustatory driver
1075 line *Gr66a*-Gal4 can be found in S- and I-type sensilla of GFP expressing GRNs.
1076 Scale bar indicates 20 µm. (D) No overlap between LacZ (green) driven by Gr5a-
1077 Gal4 and GFP (red) expressed from $fuss^{Mi13731}$/+ can be observed. (E-G) LacZ (red)
1078 expressed by *Ir76b*-Gal4 and GFP (green) expressed from $fuss^{Mi13731}$/+ overlap in L-
1079 type sensilla (arrows). Scale bars indicate 20 µm (C, D) and 25 µm (E-G),
1080 respectively. (H) Schematic representation of *fuss* expression in GRNs of L-, I- and
1081 S-type sensilla.

1082 **Fig 5. *fuss* mutant GRNs show impaired caffeine avoidance.** (A) Two-choice
1083 feeding assay reveals reduced caffeine sensation of homozygous $fuss^{Mi13731}$ and
1084 $fuss^{delDS}$ flies in contrast to their appropriate controls. As a positive control, Fuss
1085 neurons were ablated by expression of *rpr* via *fussBD*-Gal4. Transheterozygous
1086 $fuss^{delDS}/fuss^{Mi13731}$ flies also have a reduced ability to sense bitter compounds
1087 comparable to levels of homozygous $fuss^{Mi13731}$ and $fuss^{delDS}$ flies. Overexpression of
1088 *fussB* with $fuss^{delDS}$-Gal4 reduces caffeine preference to wildtype levels. Flies with a
1089 GRN specific *fuss* gene disruption (*Poxn*-Gal4-13-1 x UAS-*cas9*; UAS-*t::gRNA-*
1090 *fuss4x*) show a reduced caffeine sensation compared to controls (*Poxn*-Gal4-13-1 x
1091 UAS-*cas9*) (n=4-10 for each genotype). One-way ANOVA with *post hoc* Tukey´s test
1092 was used to calculate p-values. ****$p<0.0001$. Error bars indicate SEM. (B)
1093 Semiquantitative qPCR of bitter gustatory receptors Gr33a, Gr66a and Gr93a reveals

bioRxiv preprint doi: https://doi.org/10.1101/481721; this version posted November 29, 2018. The copyright holder for this preprint (which was not certified by peer review) is the author/funder, who has granted bioRxiv a license to display the preprint in perpetuity. It is made available under aCC-BY-ND 4.0 International license.

a reduced expression of Gr33a and Gr66a in homozygous *fuss*^{Mi13731} flies in contrast to controls. Gr93a expression of homozygous *fuss*^{Mi13731} flies is only reduced if compared to heterozygous *fuss*^{Mi13731} x WTB but not WTB flies. n=4-6 for each genotype. One-way ANOVA with *post hoc* Tukey´s test was used to calculate p-values. *p<0.05. **p<0.01. ***p<0.001. Error bars indicate SEM. (C) Analysis of Gr33a, Gr66a and Gr93a expression by semiquantitative qPCR reveals reduced expression of GRs in homozygous *fuss*^{delDS} flies in contrast to heterozygous *fuss*^{delDS} x W^{1118} and W^{1118} flies (n=4-6 for each genotype). One-way ANOVA with *post hoc* Tukey´s test was used to calculate p-values. *p<0.05 **p<0.01 ***p<0.001. Error bars indicate SEM. (D) Comparison of Fuss positive neurons and Gr33a positive neurons of the genotypes *Gr33a*-Gal4/UAS-*LacZ*;*fuss*^{Mi13731}/+ (control) and *Gr33a*-Gal4/UAS-*LacZ*;*fuss*^{Mi13731}/*fuss*^{delDS} (mutant) shows a slight reduction in Fuss positive GRN numbers (30.8 vs 28.3) and a strong reduction in Gr33a positive GRN numbers (19.4 vs 12.2). Unpaired t-test was used to calculate p-values. n=12-13 for each genotype. ***p<0.001. ****p<0.0001. Error bars indicate SEM. Adult proboscis of genotypes *Gr33a*-Gal4/UAS-*LacZ*;*fuss*^{Mi13731}/+ (control, abbr: *fuss*^{Mi13731}/+) and Gr33a-Gal4/UAS-LacZ;*fuss*^{Mi13731}/*fuss*^{delDS} (mutant, abbr: *fuss*^{Mi13731}/ *fuss*^{delDS}). Scale bar indicates 50 µm. (E) Comparison of Fuss positive neurons and Gr66a positive neurons of the genotypes UAS-*LacZ*/+;*Gr66a*-Gal4/+;*fuss*^{Mi13731}/+ (control) and UAS-*LacZ*/+;*Gr66a*-Gal4/+;*fuss*^{Mi13731}/*fuss*^{delDS} (mutant) shows a slight reduction in Fuss positive GRN numbers (30.75 vs 28.5) and an equal reduction in Gr66a positive GRN numbers (20 vs 18.3). n=12 for each genotype. Unpaired t-test was used to calculate p-values. **p<0.01. ***p<0.001. Error bars indicate SEM. Adult proboscis of genotypes UAS-*LacZ*/+;*Gr66a*-Gal4/+;*fuss*^{Mi13731}/+ (control, abbr: *fuss*^{Mi13731}/+) and UAS-*LacZ*/+;*Gr66a*-Gal4/+; *fuss*^{Mi13731}/*fuss*^{delDS} (mutant, abbr: *fuss*^{Mi13731}/ *fuss*^{delDS}). Scale bar indicates 50 µm.

bioRxiv preprint doi: https://doi.org/10.1101/481721; this version posted November 29, 2018. The copyright holder for this preprint (which was not certified by peer review) is the author/funder, who has granted bioRxiv a license to display the preprint in perpetuity. It is made available under aCC-BY-ND 4.0 International license.

1120 **Fig 6. Rpd3 interacts with Fuss and phenocopies *fuss* mutant phenotypes.** (A)
1121 Co-Immunoprecipitation experiments show that Fuss-HA binds to Rpd3-FLAG and
1122 Rpd3-HA interacts with Fuss-FLAG, respectively. No interaction between Smox and
1123 Fuss can be found regardless of the tags. (B) Knockdown of *rpd3* results in an
1124 increased preference index towards 5mM sucrose mixed with 10mM caffeine
1125 compared to *fussBD*-GAL4 x UAS-*cherry*-IR flies. n=4 for each genotype. One-way
1126 ANOVA with *post hoc* Tukey´s test was used to calculate p-values. ***p<0.001.
1127 ****p<0.001. Error bars indicate SEM. (C) Bitter gustatory receptors Gr33a, Gr66a
1128 and Gr93a are downregulated in *fussBD*-GAL4 x UAS-*rpd3*-IR flies compared to
1129 *fussBD*-GAL4 x UAS-*cherry*-IR flies. n=4-5 for each genotype. Unpaired t-test was
1130 used to calculate p-values. **p<0.01. Error bars indicate SEM.

1131 **Fig 7. Fuss is neither a regulator of Dpp signalling nor involved in mushroom**
1132 **body formation.** (A) GFP (green) expressed from heterozygous *fuss*^{Mi13731}/+ reporter
1133 line does not colocalize with pMAD (red) in larval brain. (B) GFP (green) expressed
1134 from heterozygous *fuss*^{Mi13731}/+ reporter line does not colocalize with pMAD (red) in
1135 larval VNC. (C) GFP (green) expressed from heterozygous *fuss*^{Mi13731}/+ reporter line
1136 and homozygous *fuss*^{Mi13731} marks Fuss neurons. Anti-pMAD (red) displays active
1137 Dpp signaling. No colocalization can be observed in any genotype indicating, that
1138 Fuss itself is not involved in Dpp signaling inhibition. All pictures depict slices of the
1139 larval brain or VNC and not full stacks to exclude false positive colocalization. Scale
1140 bars indicate 25 µm. (E) Representative picture of Kenyon cell nuclei of a third instar
1141 larval brain hemisphere. Nuclei of Kenyon cells are marked by colocalization of
1142 nuclear GFP driven by *OK107*-Gal4 (green, E) and EcRB1 (blue, E´´) in 3rd instar
1143 larval brains. Anti-Fuss (red, E´) staining cannot be observed in the Kenyon cell
1144 clusters. Fuss cells positive for EcRB1 expression, do not overlap with GFP
1145 expression from *OK107*-Gal4 driver (E´´´). (F-I) Mushroom bodies of an adult brain of

bioRxiv preprint doi: https://doi.org/10.1101/481721; this version posted November 29, 2018. The copyright holder for this preprint (which was not certified by peer review) is the author/funder, who has granted bioRxiv a license to display the preprint in perpetuity. It is made available under aCC-BY-ND 4.0 International license.

1146 heterozygous *fuss*^{delDS}/+ flies (F), homozygous *fuss*^{delDS} flies (G), heterozygous
1147 *fuss*^{Mi13731}/+ flies (H) and homozygous *fuss*^{Mi13731} flies (I) visualized by anti-FasII
1148 staining. (J) Ablation of Fuss neurons removes all Fuss neurons but mushroom body
1149 (red) stained with anti-Fas2 is not affected in adult brains. (K) *fussBD*-Gal4 driven
1150 UAS-*CD8-GFP* visualises projection pattern of Fuss neurons in an adult brain. (L)
1151 *fussBD*-Gal4 driven UAS-*CD8-GFP* shows Fuss neurons strongly project to lobula
1152 (white), lobula plate (red) and medulla (yellow) in an adult brain. Scale bars indicate
1153 50 µm.

1154

1155 Supporting information

1156 **S1 Fig. Characterization of *fuss*^{delDS} and *fuss*^{Mi13731} mutant flies.** (A) Genotyping
1157 of CantonS and homozygous *fuss*^{delDS} flies with fuss crispr1 seq fw and fuss crispr2
1158 seq rv oligonucleotides via PCR of genomic DNA shows reduction of around 700bp in
1159 *fuss*^{delDS} mutants as expected in contrast to control (B). Staining of heterozygous
1160 *fuss*^{delDS}/+ embryos with anti-Fuss (red) and anti-Elav (green) antibodies. Scale bar
1161 indicates 25 µm. (C,D) Staining of homozygous *fuss*^{delDS} embryos with anti-Fuss (red)
1162 and anti-Elav (green) antibodies. Scale bar indicates 25 µm. (B) Analysis of *fussB*
1163 and *fussD* transcript levels with fussBD fw and fussBD rv oligonucleotides via qPCR
1164 reveals a reduction of *fussB* and *fussD* transcript levels to 10 % in homozygous
1165 *fuss*^{Mi13731} flies in contrast to WTB flies. n=4 for each genotype. One-way ANOVA
1166 with *post hoc* Tukey´s test was used to calculate p-values. ****p<0.0001. **p<0.01.
1167 Error bars indicate SEM. (E) Anti-Fuss staining colocalizes with GFP in larval brains
1168 of heterozygous *fuss*^{Mi13731}/+ line. (F) No anti-Fuss staining in larval brains of
1169 homozygous *fuss*^{Mi13731} line can be detected. Arrowhead indicates magnified cell
1170 cluster. (G) Location of the four CRISPR target sites of the UAS-*t::gRNA-fuss*^{4x}

bioRxiv preprint doi: https://doi.org/10.1101/481721; this version posted November 29, 2018. The copyright holder for this preprint (which was not certified by peer review) is the author/funder, who has granted bioRxiv a license to display the preprint in perpetuity. It is made available under aCC-BY-ND 4.0 International license.

1171 construct in the DNA sequence of the Ski/Sno homology domain. (H) Adult brains of
1172 UAS-*cas9*/UAS-*fussB-GFP*; *fussBD*-Gal4/+ flies show normal Fuss expression
1173 pattern- Scale bar indicates 50 µm. (I) In flies of the genotype UAS-*cas9*/UAS-*fussB-*
1174 *GFP*; UAS-*t::gRNA-fuss*^{4x}*; fussBD*-Gal4/+ fussB-GFP is strongly reduced. Scale bar
1175 indicates 50 µm.

1176 **S2 Fig. Characterization of anti-Fuss antibody and Fuss neurons.** (A) Schematic
1177 representation of conserved domains and localization of the Fuss16 fragment used
1178 for immunization. Exact sequence of Fuss16-His fragment shown in red. (B)
1179 Detection of Fuss-GFP (green) from heatshock induced Fuss-GFP flies in western
1180 blots by anti-GFP and anti-Fuss antibodies. As a negative control CantonS is used
1181 and Tubulin as a housekeeper protein (red). Both antibodies recognize a predicted
1182 protein size of 112 kDa for the fusion protein. Endogenous levels of the Fuss protein
1183 cannot be detected on western blots due to the low abundance of the protein. (C)
1184 Comparison of VNC of stage 13 embryo with VNC of stage 16 embryo shows
1185 increase in number of Fuss (green) or Toy (red) cells, but only one cell per
1186 hemineuromer shows colocalization of both markers. (D) Comparison of expression
1187 pattern of interneuron marker Engrailed (red) and Fuss (green) visualized by antibody
1188 staining in embryonic VNC. (E) Fuss expression pattern as revealed by expression of
1189 GFP (green) by heterozygous *fuss*^{Mi13731}/+ in larval brains does not colocalize with
1190 LacZ (red) driven by *Hb9*-GAL4 line. (F) Even skipped (red), a motor neuron marker,
1191 is not expressed in Fuss neurons (green) visualized by antibody staining in
1192 embryonic VNC. (G) Ventral Apterous cells marked by expression of CD8-RFP (red)
1193 with *ap*-Gal4 are positive for Fuss (green) expression in larval VNC. Scale bars
1194 indicate 30 µm (C, D, E, F) and 10 µm (G).

bioRxiv preprint doi: https://doi.org/10.1101/481721; this version posted November 29, 2018. The copyright holder for this preprint (which was not certified by peer review) is the author/funder, who has granted bioRxiv a license to display the preprint in perpetuity. It is made available under aCC-BY-ND 4.0 International license.

1195 **S3 Fig. Fuss is not expressed in adult insulin like producing cells or**
1196 **dopaminergic neurons as revealed by TaDa and immunostainings.** (A) *pale* (*ple*)
1197 is weakly bound by Dam-PolII as revealed by TaDa and no colocalization is observed
1198 between Ple positive cells (red) and GFP expressed by the heterozygous
1199 *fuss*^{Mi13731}/+ reporter line (green) in whole adult brains. Overlap between signals
1200 arises from different optical slices and not from colocalization. (B) *insulin like peptide*
1201 *2* (*ilp2)* is weakly bound by Dam-PolII as revealed by TaDa. Confocal slices covering
1202 the pars intercerebralis and a part of the adult brain hemisphere show no
1203 colocalization between insulin producing cells labeled with anti-Ilp2 antibody (red)
1204 and Fuss neurons labeled with anti-Fuss antibody (green). In (A) and (B) regions
1205 bound stronger by Dam-PolII than by Dam are depicted in green, whereas regions
1206 bound stronger by Dam than by Dam-PolII are depicted in red. Scale bars indicate 50
1207 µm.

1208 **S4 Fig. *fuss* mutant flies show an impaired bitter taste sensation.** (A) Expression
1209 of UAS-*CD8-GFP* with *fussBD*-Gal4 reveals four GRNs located in the two last tarsal
1210 segments of the prothoracic, mesothoracic and metatoracic leg. Scale bars indicate
1211 50 µm. (B) GFP expression from *Poxn*-Gal4-13-1 is not overlapping with Cherry
1212 expression from *fuss*$^{Mi\text{-}cherry}$ reporter line in neurons of the adult CNS. Overlap can
1213 only be observed in GRN nerve fibers from proboscis. EBN = ellipsoid body neurons.
1214 ALI = Antennal lobe interneurons. Scale bar indicates 50 µm. (C) Homozygous
1215 *fuss*^{Mi13731} flies show reduced caffeine sensation also at lower concentrations
1216 compared to heterozygous *fuss*^{Mi13731} x WTB and WTB flies. n=4-9 for each
1217 genotype. One-way ANOVA with *post hoc* Tukey´s test was used to calculate p-
1218 values. **p<0.01 ****p<0.0001. Error bars indicate SEM. (D) Homozygous *fuss*^{Mi13731}
1219 mutant flies show reduced sensation of denatonium benzoate compared to
1220 heterozygous *fuss*^{Mi13731} x WTB and WTB flies at a concentration of 100 µm. At 500

bioRxiv preprint doi: https://doi.org/10.1101/481721; this version posted November 29, 2018. The copyright holder for this preprint (which was not certified by peer review) is the author/funder, who has granted bioRxiv a license to display the preprint in perpetuity. It is made available under aCC-BY-ND 4.0 International license.

1221 µm denatonium benzoate effect of homozygous *fuss*^{Mi13731} flies is reversed to control
1222 levels. n=4-5 for each genotype. One-way ANOVA with *post hoc* Tukey´s test was
1223 used to calculate p-values. ****p<0.0001. Error bars indicate SEM. (E)
1224 Transheterozygous *fuss*^{Mi13731}/*fuss*^{delDS} mutants show reduced transcript levels fo
1225 Gr33a, Gr66a and Gr93a in contrast to W^{1118} control. n=4 for each genotype. One-
1226 way ANOVA with *post hoc* Tukey´s test was used to calculate p-values. ***p<0.001.
1227 **p<0.01. *p<0.05. Error bars indicate SEM. (F) Alignment of *Drosophila* Fuss with
1228 mouse Skor1 and Skor2. Ski/Sno/Dac homology domain, SMAD4 binding domain
1229 and proposed Rpd3 interaction fragment in Skor2 are displayed by colored lines as
1230 described.

1231 **S1 Appendix. Average PolII occupancy and FDR of control dataset.**

1232 **S2 Appendix. Average PolII occupancy and FDR of mutant dataset.**

1233 **S3 Appendix. Data for generating graphs.**

1234

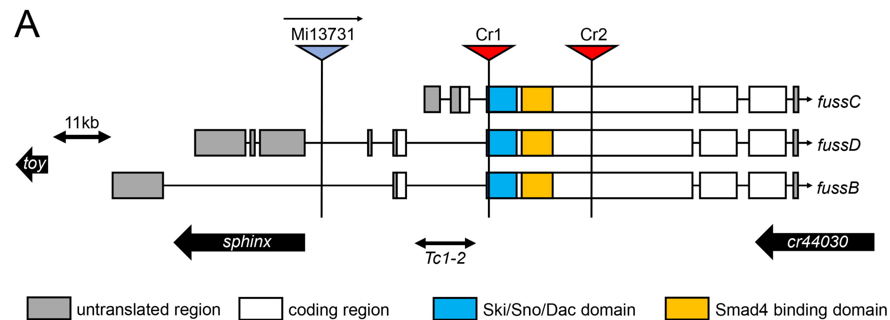
A
Mi13731
Cr1
Cr2
fussC
fussD
fussB
11kb
toy
sphinx
Tc1-2
cr44030
untranslated region
coding region
Ski/Sno/Dac domain
Smad4 binding domain

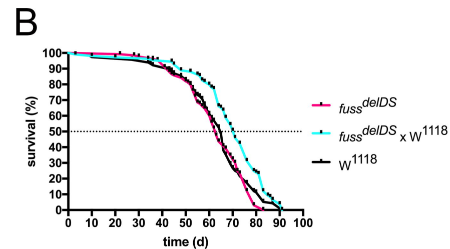
B
survival (%)
time (d)
fussdelDS
fussdelDS x W1118
W1118

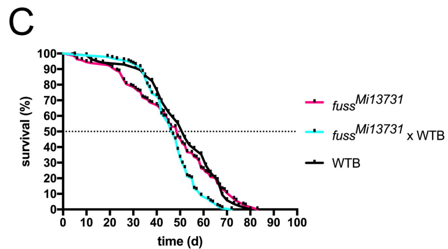
C
survival (%)
time (d)
fussMi13731
fussMi13731 x WTB
WTB

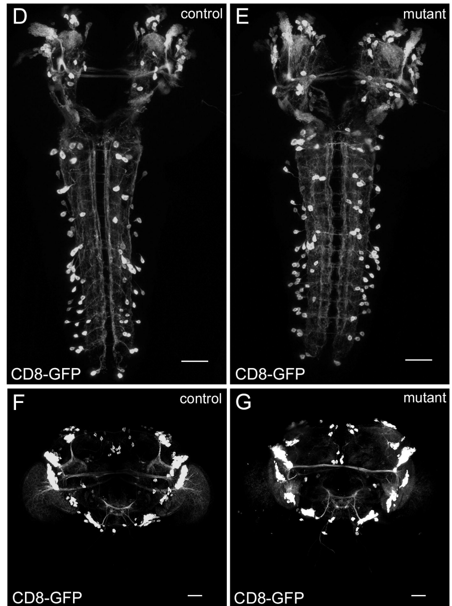
D
control
E
mutant
CD8-GFP
CD8-GFP
F
control
G
mutant
CD8-GFP
CD8-GFP

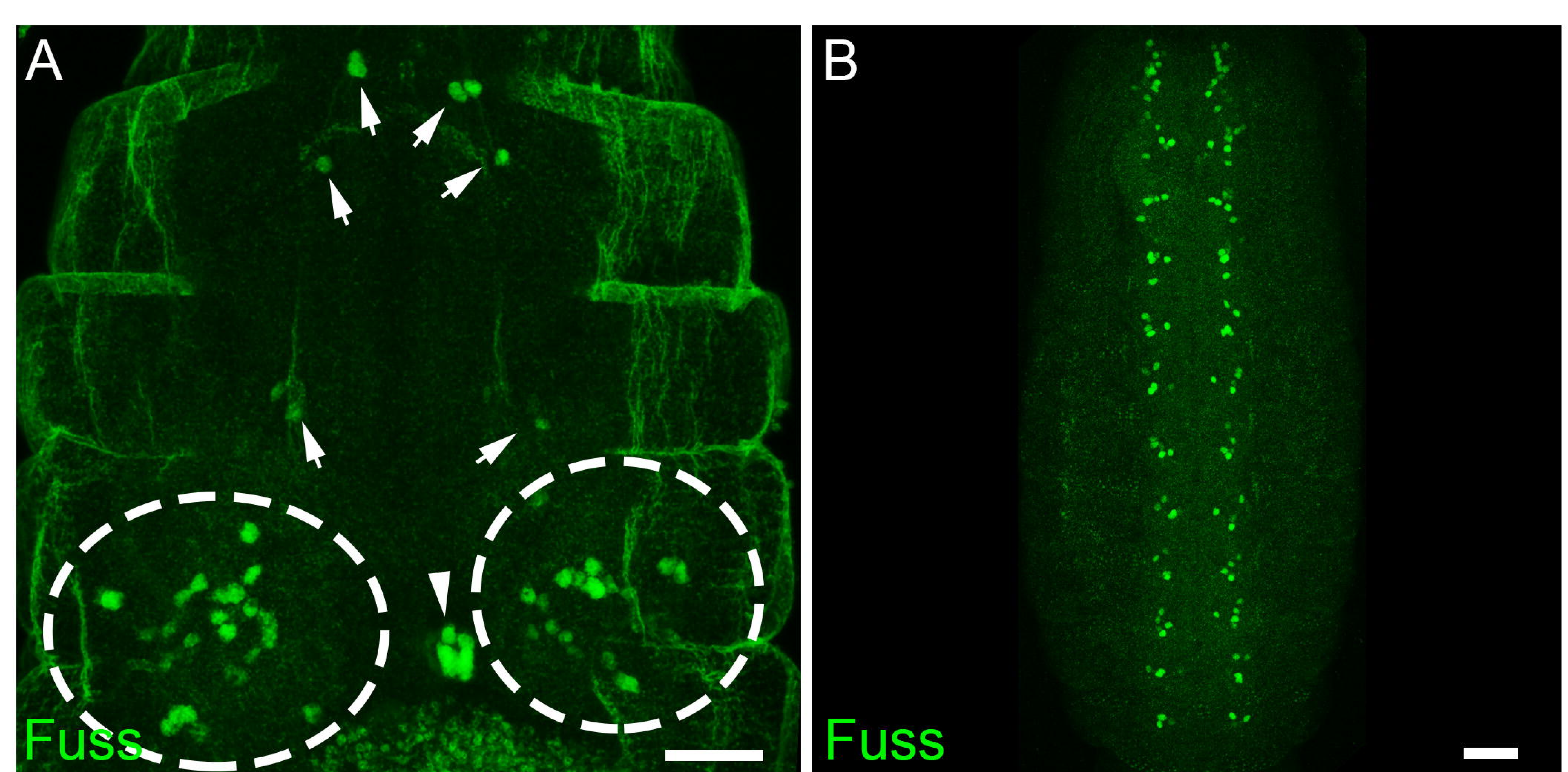
A
B
Fuss
Fuss
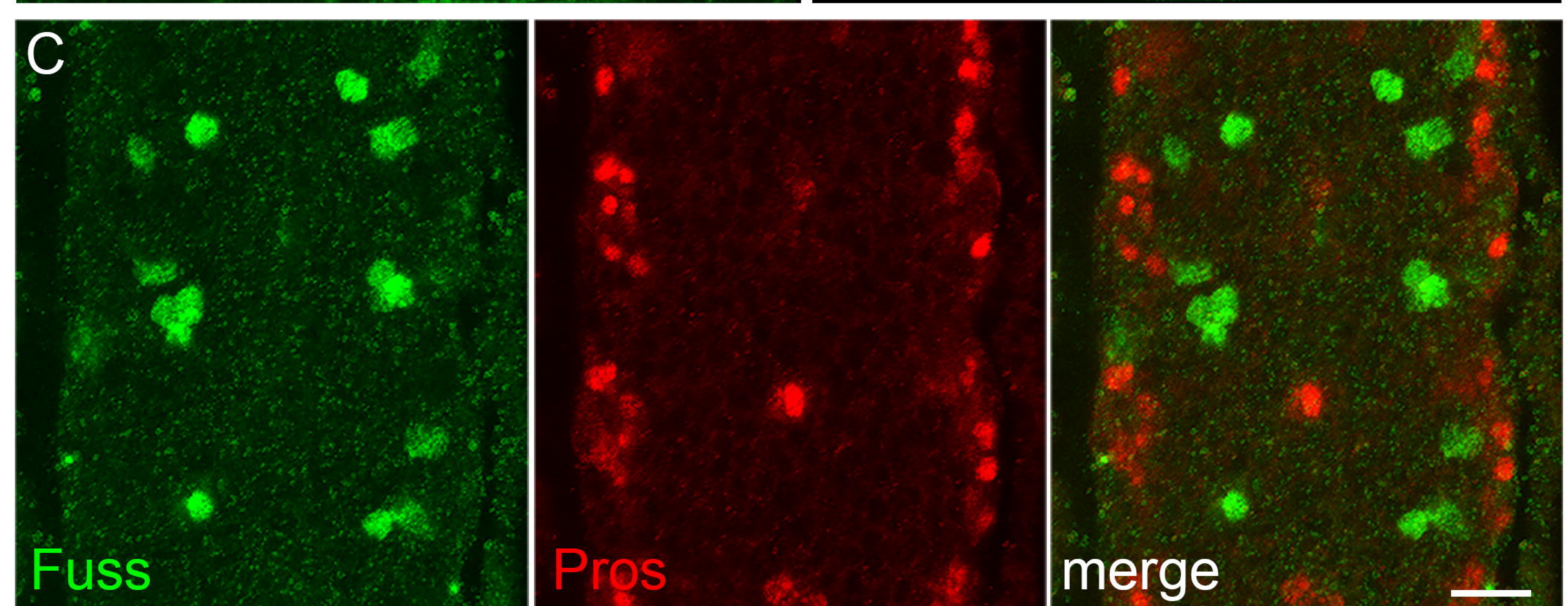
C
Fuss
Pros
merge
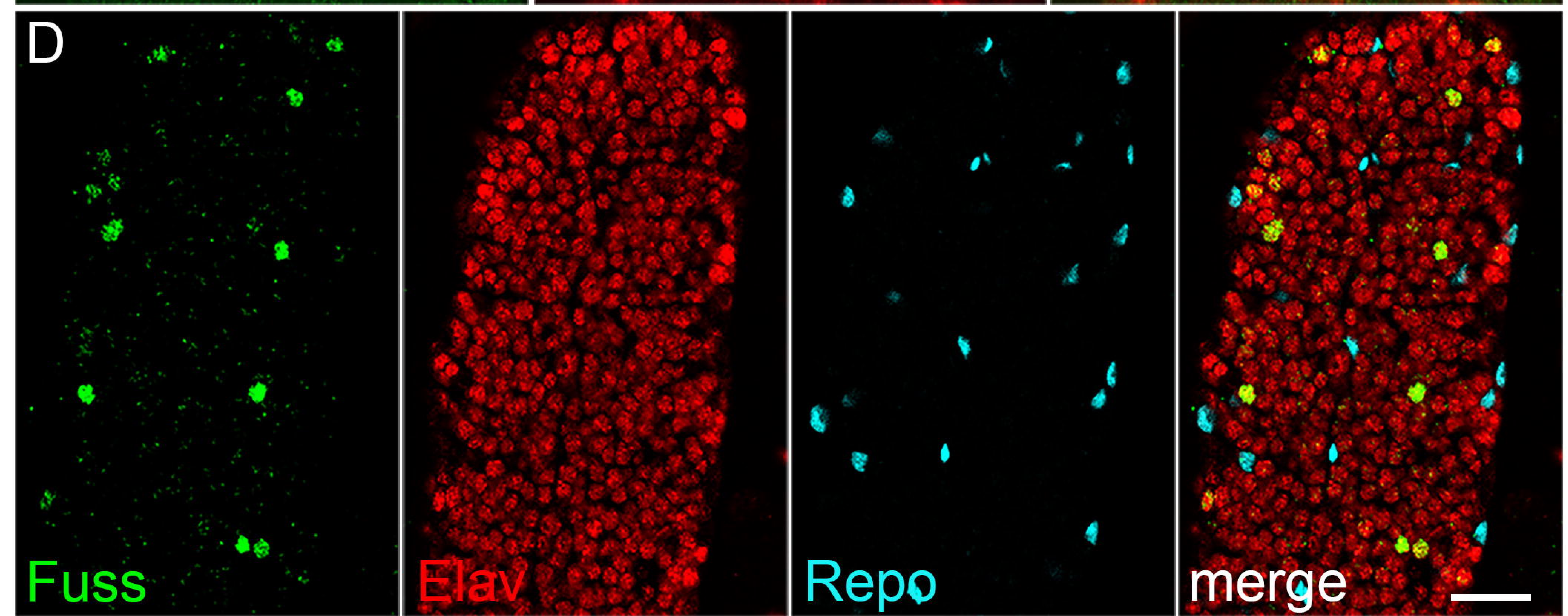
D
Fuss
Elav
Repo
merge
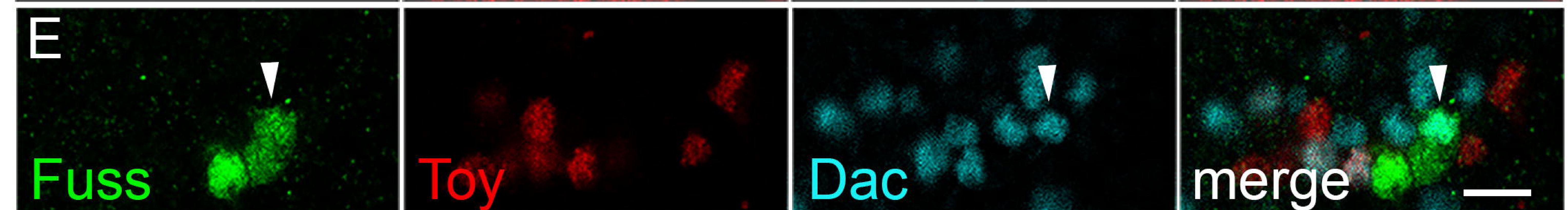
E
Fuss
Toy
Dac
merge
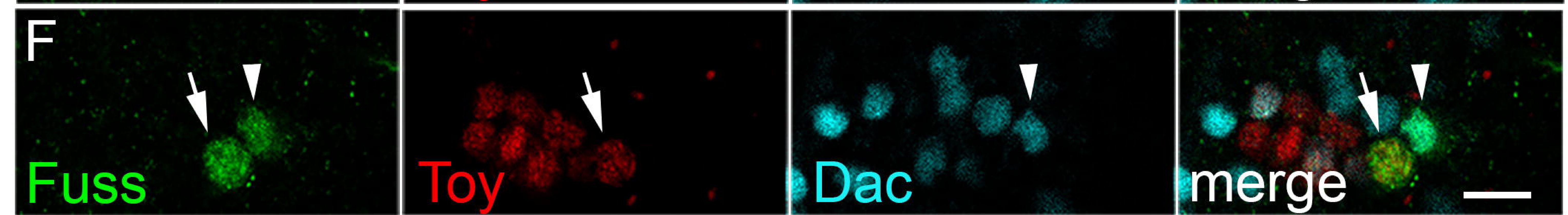
F
Fuss
Toy
Dac
merge
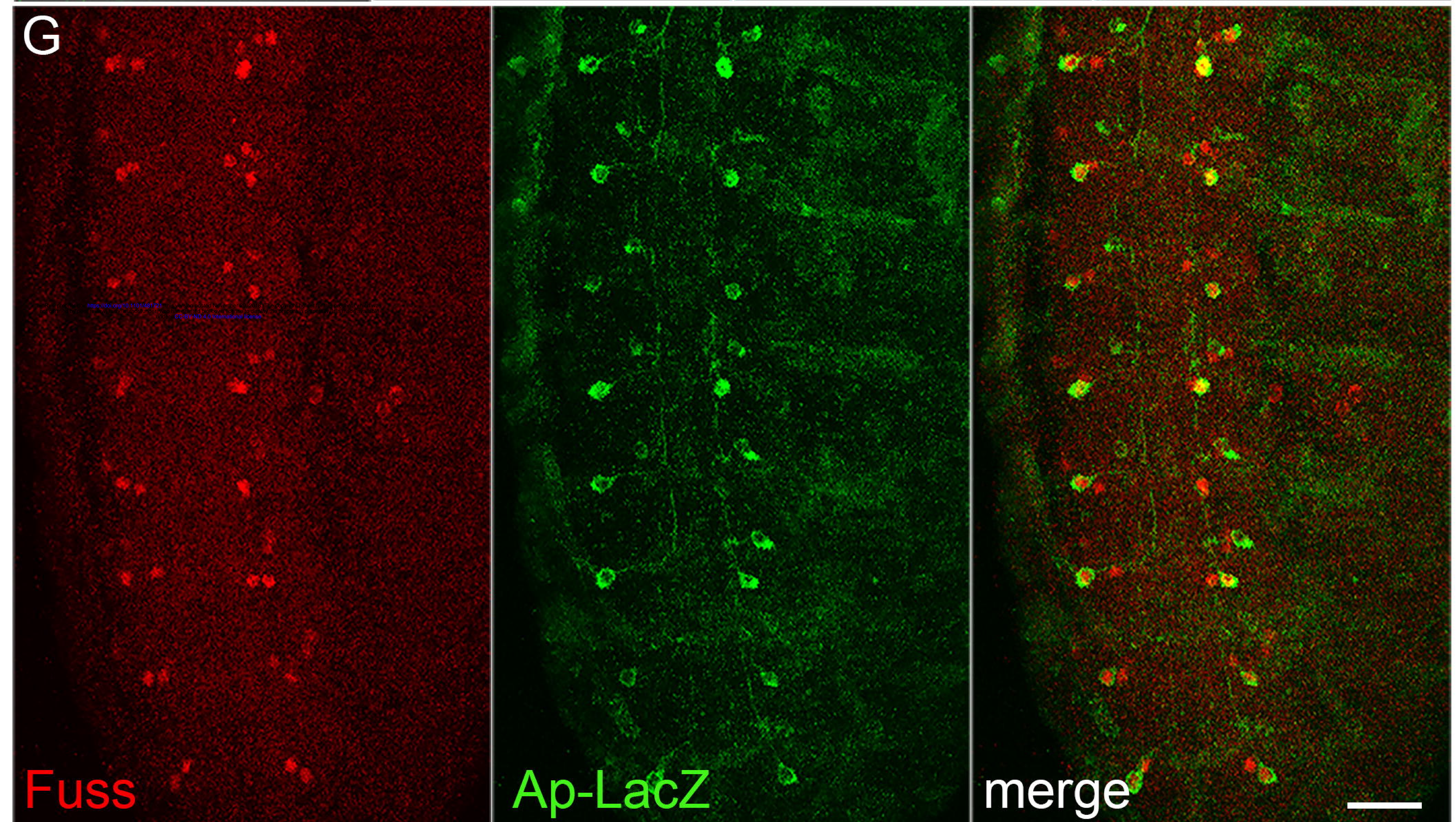
G
Fuss
Ap-LacZ
merge

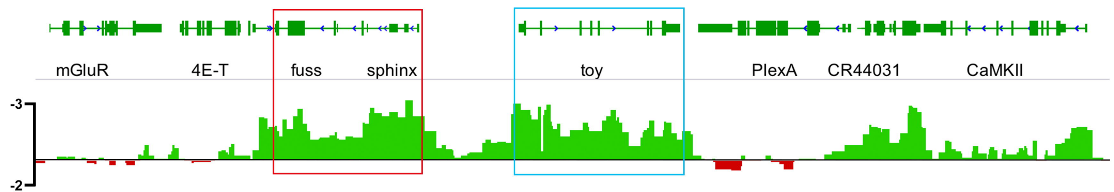
A
Chr 4
mGluR
4E-T
fuss
sphinx
toy
PlexA
CR44031
CaMKII
-3
-2

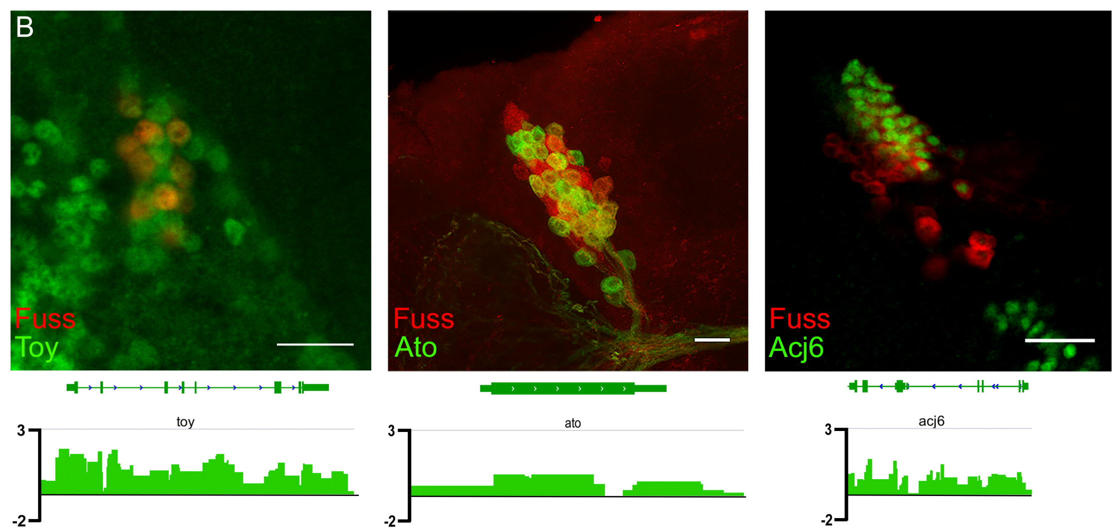
B
Fuss
Toy
Fuss
Ato
Fuss
Acj6
toy
ato
acj6
3
-2

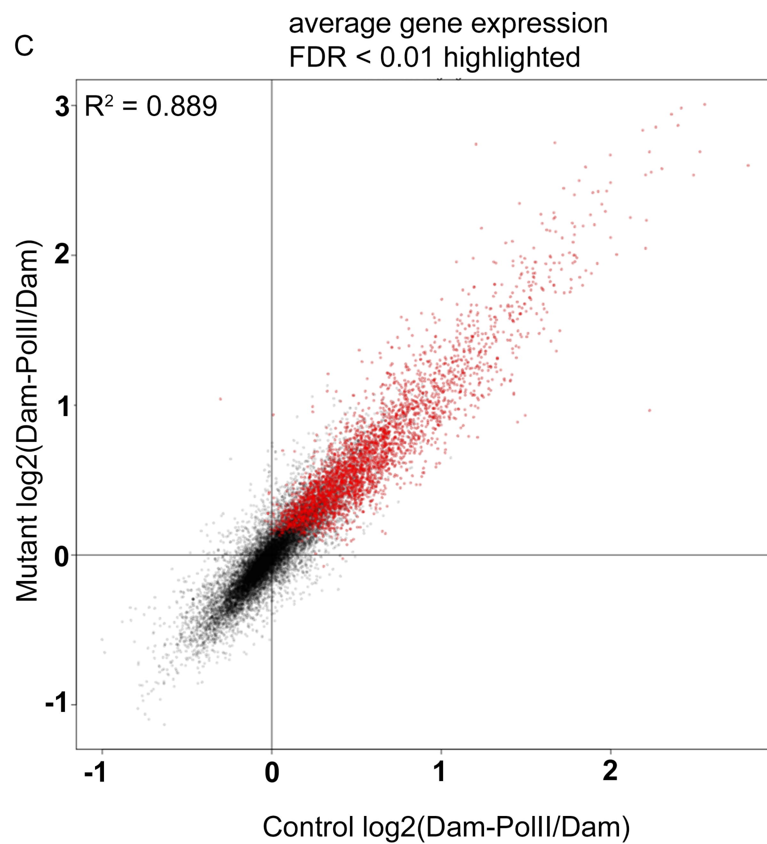
C
average gene expression
FDR < 0.01 highlighted
R^2 = 0.889
Mutant log2(Dam-PolII/Dam)
Control log2(Dam-PolII/Dam)
3
2
1
0
-1

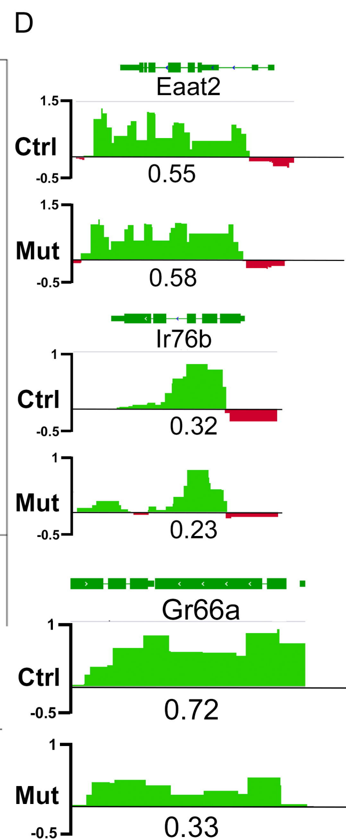
D
Eaat2
Ctrl
0.55
Mut
0.58
Ir76b
Ctrl
0.32
Mut
0.23
Gr66a
Ctrl
0.72
Mut
0.33
1.5
1
-0.5

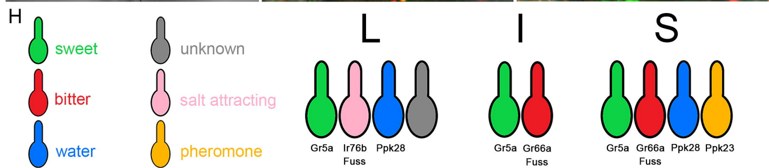
A
PPS
Fuss
Gr33a
merge
DPO
Fuss
Gr33a
merge
DPS
Fuss
Gr33a
merge
B
DPS
Fuss
Gr93a
merge
C
Fuss
Gr66a
merge
D
Fuss
Gr5a
merge
E
Fuss
Ir76b
F
Fuss
Ir76b
G
Fuss
Ir76b
H
sweet
bitter
water
unknown
salt attracting
pheromone
L
Gr5a
Ir76b
Fuss
Ppk28
I
Gr5a
Gr66a
Fuss
S
Gr5a
Gr66a
Fuss
Ppk28
Ppk23

A

5mM sucrose + 10mM caffeine

preference index

1mM sucrose

fussBD-Gal4 x UAS-gfp
fussBD-Gal4 x UAS-rpr
W1118
fussdelDS x W1118
fussdelDS
WTB
fussMi13731 x WTB
fussMi13731
fussMi13731 x fussdelDS
fussdelDS-Gal4 x UAS-Stinger; fussdelDS
fussdelDS-Gal4 x UAS-fussB; fussdelDS
Poxn-Gal4-13-1 x UAS-cas9
Poxn-Gal4-13-1 x UAS-cas9; UAS-t::gRNA-fuss4x

B

Gr33a
Gr66a
Gr93a

expression level

WTB
fussMi13731 x WTB
fussMi13731

C

Gr33a
Gr66a
Gr93a

expression level

W1118
fussdelDS x W1118
fussdelDS

D

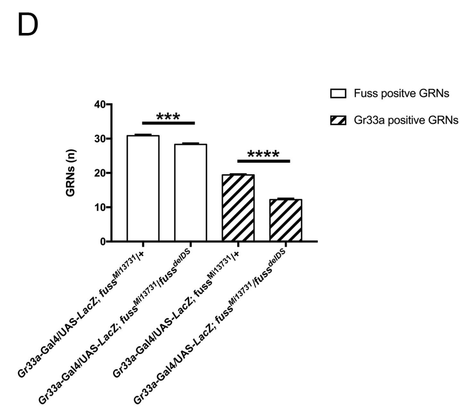

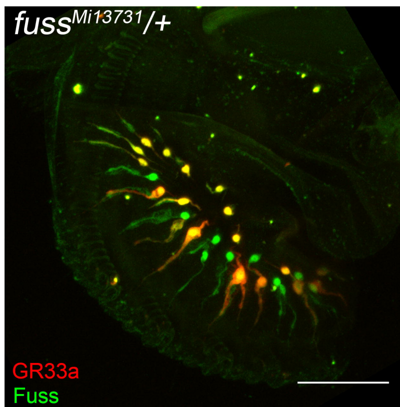

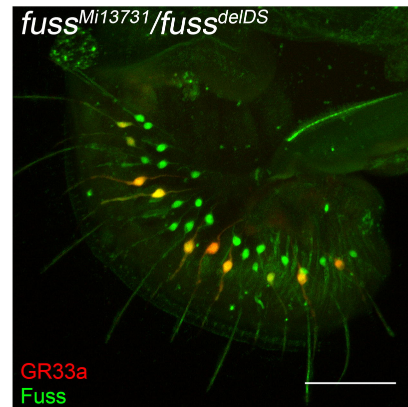

E

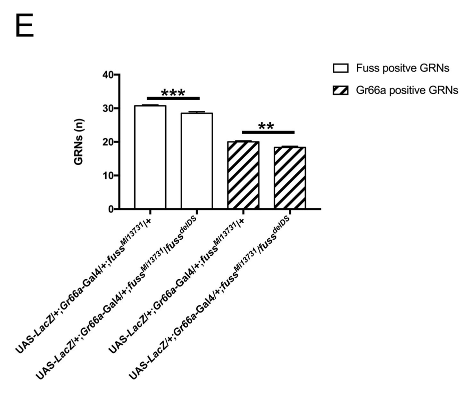

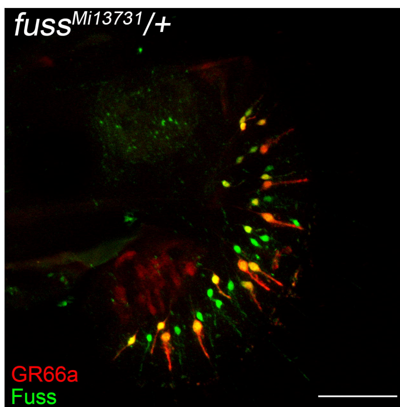

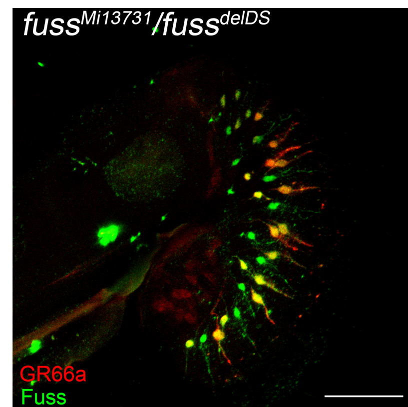

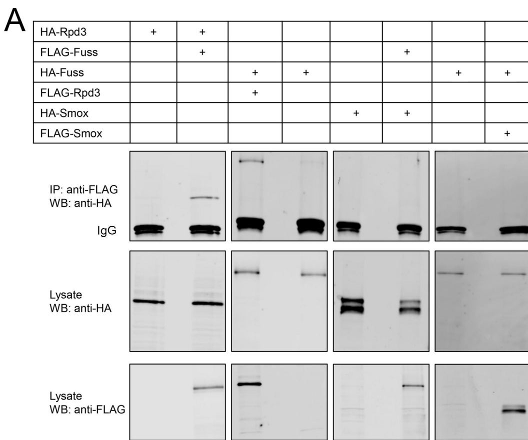
A
HA-Rpd3
FLAG-Fuss
HA-Fuss
FLAG-Rpd3
HA-Smox
FLAG-Smox
IP: anti-FLAG
WB: anti-HA
IgG
Lysate
WB: anti-HA
Lysate
WB: anti-FLAG

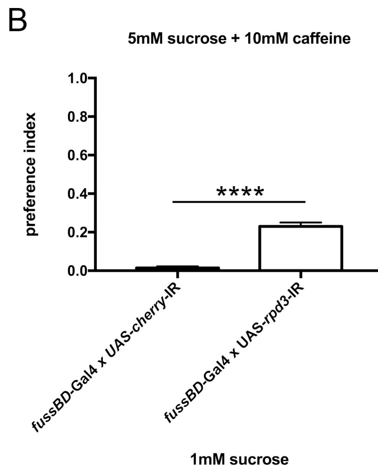
B
5mM sucrose + 10mM caffeine
preference index
1.0
0.8
0.6
0.4
0.2
0.0
****
fussBD-Gal4 x UAS-cherry-IR
fussBD-Gal4 x UAS-rpd3-IR
1mM sucrose

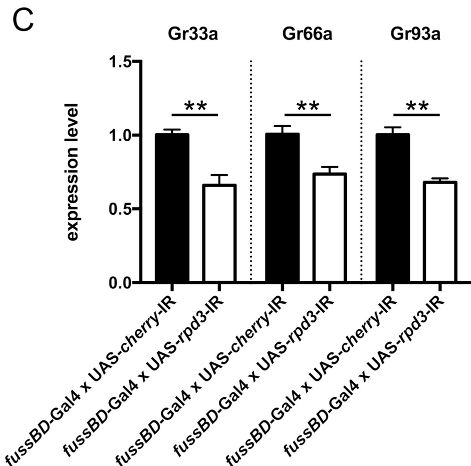
C
Gr33a
Gr66a
Gr93a
expression level
1.5
1.0
0.5
0.0
**
**
**
fussBD-Gal4 x UAS-cherry-IR
fussBD-Gal4 x UAS-rpd3-IR
fussBD-Gal4 x UAS-cherry-IR
fussBD-Gal4 x UAS-rpd3-IR
fussBD-Gal4 x UAS-cherry-IR
fussBD-Gal4 x UAS-rpd3-IR

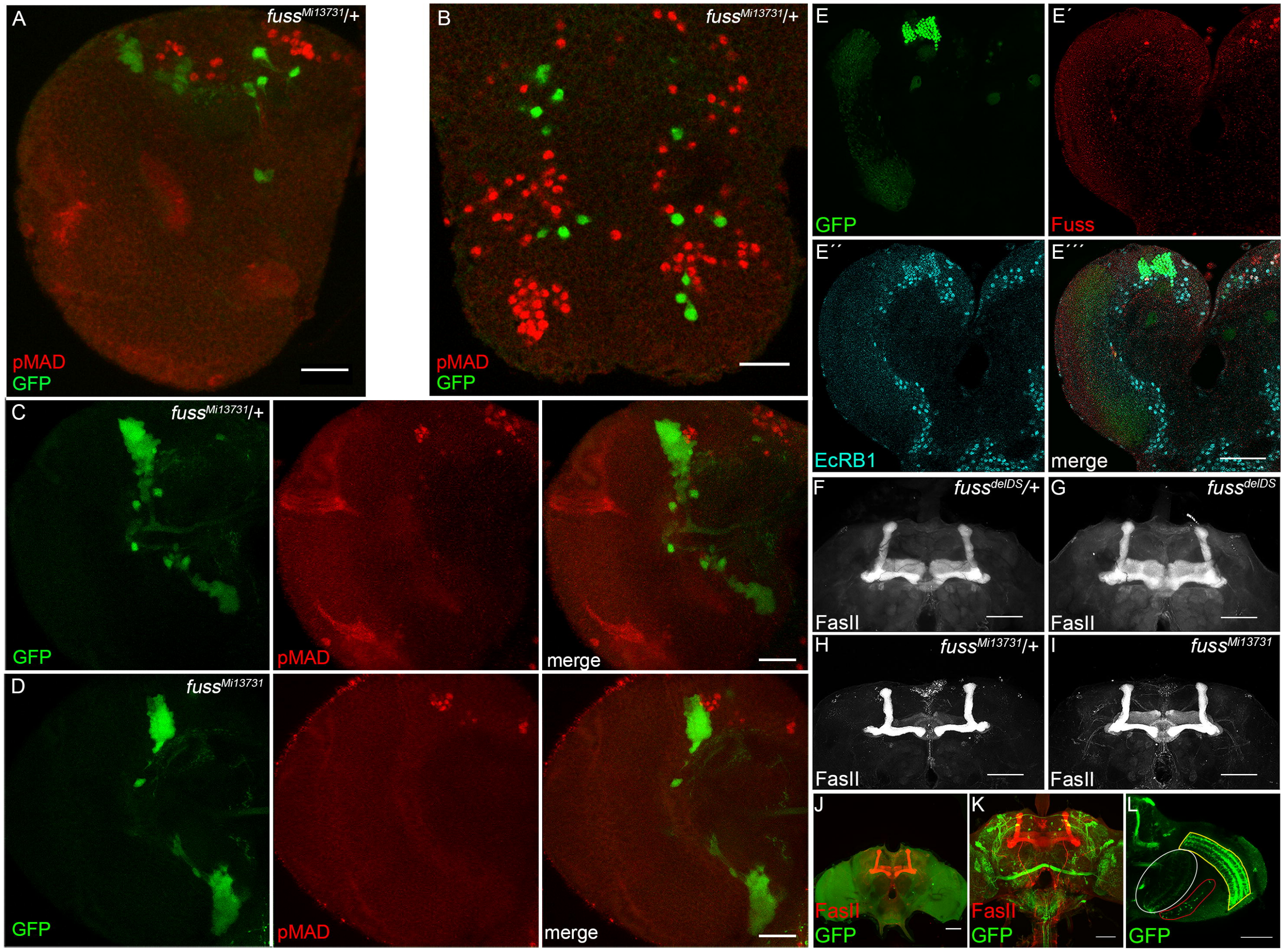

A
fussMi13731/+
pMAD
GFP
B
fussMi13731/+
pMAD
GFP
C
fussMi13731/+
GFP
pMAD
merge
D
fussMi13731
GFP
pMAD
merge
E
GFP
E´
Fuss
E´´
EcRB1
E´´´
merge
F
fussdelDS/+
FasII
G
fussdelDS
FasII
H
fussMi13731/+
FasII
I
fussMi13731
FasII
J
FasII
GFP
K
FasII
GFP
L
GFP